Ror2 regulates branching, differentiation, and actin-cytoskeletal dynamics within the mammary epithelium

Kevin Roarty,[1] Amy N. Shore,[1] Chad J. Creighton,[2] and Jeffrey M. Rosen[1]

[1]Department of Molecular and Cellular Biology and [2]Dan L. Duncan Cancer Center, Baylor College of Medicine, Houston, TX 77030

Wnt signaling encompasses β-catenin–dependent and –independent networks. How receptor context provides Wnt specificity in vivo to assimilate multiple concurrent Wnt inputs throughout development remains unclear. Here, we identified a refined expression pattern of Wnt/receptor combinations associated with the Wnt/β-catenin–independent pathway in mammary epithelial subpopulations. Moreover, we elucidated the function of the alternative Wnt receptor Ror2 in mammary development and provided evidence for coordination of this pathway with Wnt/β-catenin–dependent signaling in the mammary epithelium. Lentiviral short hairpin RNA (shRNA)-mediated depletion of Ror2 in vivo increased branching and altered the differentiation of the mammary epithelium. Microarray analyses identified distinct gene level alterations within the epithelial compartments in the absence of Ror2, with marked changes observed in genes associated with the actin cytoskeleton. Modeling of branching morphogenesis in vitro defined specific defects in cytoskeletal dynamics accompanied by Rho pathway alterations downstream of Ror2 loss. The current study presents a model of Wnt signaling coordination in vivo and assigns an important role for Ror2 in mammary development.

Introduction

The mammary gland exhibits extensive proliferative and differentiation potential throughout development. In particular, ductal extension and branching during puberty and epithelial expansion of alveolar milk-forming units within pregnancy require distinct morphological movements and coordinated efforts of multiple epithelial constituents within basal and luminal compartments of the bilayered mammary tree (Macias and Hinck, 2012). Epithelial lineages are derived from a hierarchical network of stem, progenitor, and more differentiated progeny. Stem cells are capable of giving rise to all lineages of the ductal network upon transplantation (Shackleton et al., 2006; Stingl et al., 2006), and as indicated by lineage tracing, generate both myoepithelial and luminal epithelial lineages during periods of active ductal growth and maintenance (Van Keymeulen et al., 2011; van Amerongen et al., 2012a; Rios et al., 2014; Wang et al., 2014). Bulb-shaped terminal end buds (TEBs) drive development during puberty, where an outer layer of stem-like cap cells and an inner layer of body cells lay the foundation for the epithelial constituents that make up the ductal network (Smalley and Ashworth, 2003; Srinivasan et al., 2003).

Wnt/β-catenin signaling is essential for orchestrating self-renewal cues required for stem cell maintenance and cell fate decisions in multiple embryonic and postnatal tissues (Zeng and Nusse, 2010; van Amerongen et al., 2012a). The Wnt/β-catenin pathway is required at the earliest stage of mammary development in the embryo for the specification of the mammary placode and initiation of mammary morphogenesis (Chu et al., 2004) and in postnatal development for proper stem cell maintenance, branching morphogenesis, and alveolar development (Hatsell et al., 2003; Lindvall et al., 2006; Badders et al., 2009). Pathway activation occurs through the binding of a Wnt ligand to a receptor complex composed of Frizzled (Fzd) and a coreceptor low-density lipoprotein receptor-related protein 5 or 6 (LRP5/6). This Wnt–receptor combination prompts the disassociation of a complex composed of glycogen synthase kinase 3 (GSK3), casein kinase 1α (CK1α), Axin, and adenomatous

Correspondence to Jeffrey M. Rosen: jrosen@bcm.edu

Abbreviations used in this paper: AP, alveolar progenitor; APC, adenomatous polyposis coli; CDC42, cell division cycle 42; DIC, differential interference contrast; ERM, ezrin/radixin/moesin; FGF, fibroblast growth factor; Fzd, Frizzled; IF, immunofluorescence; Lrp5/6, low-density lipoprotein receptor-related protein 5/6; LP, luminal progenitor; MEC, mammary epithelial cell; ML, mature luminal; NKCC1, Na-K-Cl cotransporter 1; qRT-PCR, quantitative RT-PCR; s-SHIP, SH2-containing inositol 5″-phosphate; TEB, terminal end bud; ZO-1, Zona occludens protein 1.

The Rockefeller University Press $30.00
J. Cell Biol. Vol. 208 No. 3 351–366
www.jcb.org/cgi/doi/10.1083/jcb.201408058

polyposis coli (APC), resulting in stabilization of β-catenin (Angers and Moon, 2009).

The Wnt/β-catenin–independent pathway embodies alternative Wnt signaling mechanisms that do not stabilize β-catenin or engage the coreceptors LRP5/6. Rather, these outcomes control various processes such as planar cell polarity, convergent extension, calcium fluxes, and actin/cytoskeletal rearrangements (Angers and Moon, 2009). Relative to the Wnt/β-catenin pathway, the molecular determinants of Wnt/β-catenin–independent pathways are less characterized; however, proteins implicated in Wnt/β-catenin–independent pathways include the Rho and Rac GTPases, Rho-Kinase (ROCK), c-Jun-N-terminal kinase (JNK), and the calcium-sensitive enzymes PKC and calcium/calmodulin-dependent protein kinase type II (CAMKII; van Amerongen et al., 2008, 2012; Angers and Moon, 2009). Implicit in conveying the specificity of Wnt signaling transduction, the Wnt receptor repertoire likely plays an instrumental role in assimilating multiple concurrent Wnt inputs within a developmental context (van Amerongen and Nusse, 2009).

Alternative receptors of the Ror and Ryk receptor tyrosine kinase families are mediators of Wnt/β-catenin–independent signaling together with Fzd receptors. Ror1 and Ror2 display both overlapping and distinct spatiotemporal expression patterns in the developing embryo (Matsuda et al., 2001). Interestingly, Wnt5a and Ror2 exhibit overlapping spatiotemporal expression in multiple embryonic structures, and strong phenotypic similarities exist between mice deficient in Ror2 and Wnt5a (Yamaguchi et al., 1999; DeChiara et al., 2000; Takeuchi et al., 2000). Multiple models have since established that Ror2 mediates Wnt5a signaling, and under certain contexts, results in the antagonism of the Wnt/β-catenin pathway (Mikels and Nusse, 2006; van Amerongen et al., 2012b). Although functions for the Wnt5a/Ror axis have been established based on phenotypic defects in *Caenorhabditis elegans*, *Xenopus laevis*, and vertebrates, exactly how multiple cell types within a given tissue convey specific Wnt signals to coordinate a particular developmental process remains unknown. In the mammary gland, the existence of multiple Wnt ligands has been realized for decades (Gavin and McMahon, 1992; Bühler et al., 1993); however, the contribution of the receptor to Wnt signaling specificity and function in vivo remains undefined.

We therefore interrogated the developmental outcome of Ror2 loss in the postnatal mammary gland by lentiviral-mediated shRNA silencing. Using this approach, we observed that disruption of Ror2 in vivo affects branching and differentiation of the mammary epithelium. Gene expression profiling of sorted epithelial fractions revealed distinct alterations within luminal and basal epithelial compartments in Ror2-deficient mammary outgrowths. Notably, dramatic changes in actin cytoskeletal genes affecting mammary developmental outcome were detected. We also examined the integration of Wnt/β-catenin–dependent and –independent signaling machinery as it relates to the epithelial hierarchy and coordination of tissue morphogenesis. Collectively, this study uncovers an intricate model of Wnt pathway coordination in vivo and assigns an important role for the alternative Wnt receptor Ror2 in directing branching morphogenesis, differentiation, and actin-cytoskeletal cues within the mammary epithelium.

Results

Ligands and receptors of the Wnt/β-catenin–independent pathway exhibit temporal and spatial regulation in the mammary gland

Discovery of the expression of multiple Wnt ligands in the mammary gland suggested the necessity for these proteins in the regulation of mammary gland development (Gavin and McMahon, 1992; Bühler et al., 1993). To gain a better understanding of the specificity of Wnt signaling in the context of mammary development, we sought to identify the spatiotemporal expression patterns of Wnt ligand and receptor components within the mammary epithelium. Using FACS, we isolated bulk luminal ($CD24^+CD29^{lo}$) and basal ($CD24^+CD29^{hi}$) epithelial cell fractions from 8-wk virgin, and 10.5- and 17.5-d pregnant stages of development to assess expression levels of Wnt ligand and receptor constituents across different stages of development (Fig. 1 A). Quantitative RT-PCR (qRT-PCR) analysis of *Keratin 8* (K8) and *Keratin 14* (K14) markers confirmed the purity of sorted populations (Fig. S1, A and B). We determined that multiple Wnt ligands exist in mammary epithelial compartments, displaying a spectrum of luminal-enriched (*Wnt4*, *Wnt5a*), basal-enriched (*Wnt6*), and neutral (*Wnt5b*, *Wnt7b*) expression patterns (Fig. 1 B and Fig. S1 C). Given that certain Wnts activate Wnt/β-catenin responses and others engage Wnt/β-catenin–independent responses, components of the less-characterized Wnt/β-catenin–independent arm of signaling were further explored.

Interestingly, when assessing expression of the noncanonical Wnt receptors *Ror1* and *Ror2*, we discovered similar patterns of expression between *Wnt5a* and *Ror2* as well as *Wnt5b* and *Ror1* (Fig. 1, B and C). Specifically, *Wnt5a/Ror2* expression decreased during pregnancy in luminal cells, whereas *Wnt5b/Ror1* expression increased. Expression patterns of Wnts and their associated receptors were subsequently assessed in more refined epithelial subpopulations. Studies have demonstrated the ability to segregate the luminal $CD24^+CD29^{lo}$ fraction into mature luminal (ML; $c\text{-}kit^-CD14^-$), luminal progenitor (LP; $c\text{-}kit^+CD14^+$), and alveolar progenitor (AP; $c\text{-}kit^{-/lo}CD14^+$) subpopulations based on the expression of c-kit and CD14b (Asselin-Labat et al., 2011). These subpopulations were FACS sorted for downstream expression analysis and validated by qRT-PCR (Shore et al., 2012). Intriguingly, when expression patterns of *Wnt5a/Ror2* and *Wnt5b/Ror1* were evaluated within the luminal fractions, they exhibited similar expression trends, with *Wnt5a/Ror2* present in ML and LP cell subpopulations and *Wnt5b/Ror1* present in LP and AP subsets (Fig.1, D and E). In the luminal fractions specifically, the similarity in expression trends of individual ligand–receptor pairs suggests the existence of autocrine Wnt/β-catenin–independent signaling. *Ror1* and *Ror2* were additionally expressed in the basal cell layer, highlighting the presence of paracrine signaling mechanisms as well. These observations suggest a yet-undefined role for β-catenin–independent Wnt signaling in mammary epithelial homeostasis and offer insight into the potential Wnt ligand/receptor pairings exhibited in the mammary epithelium.

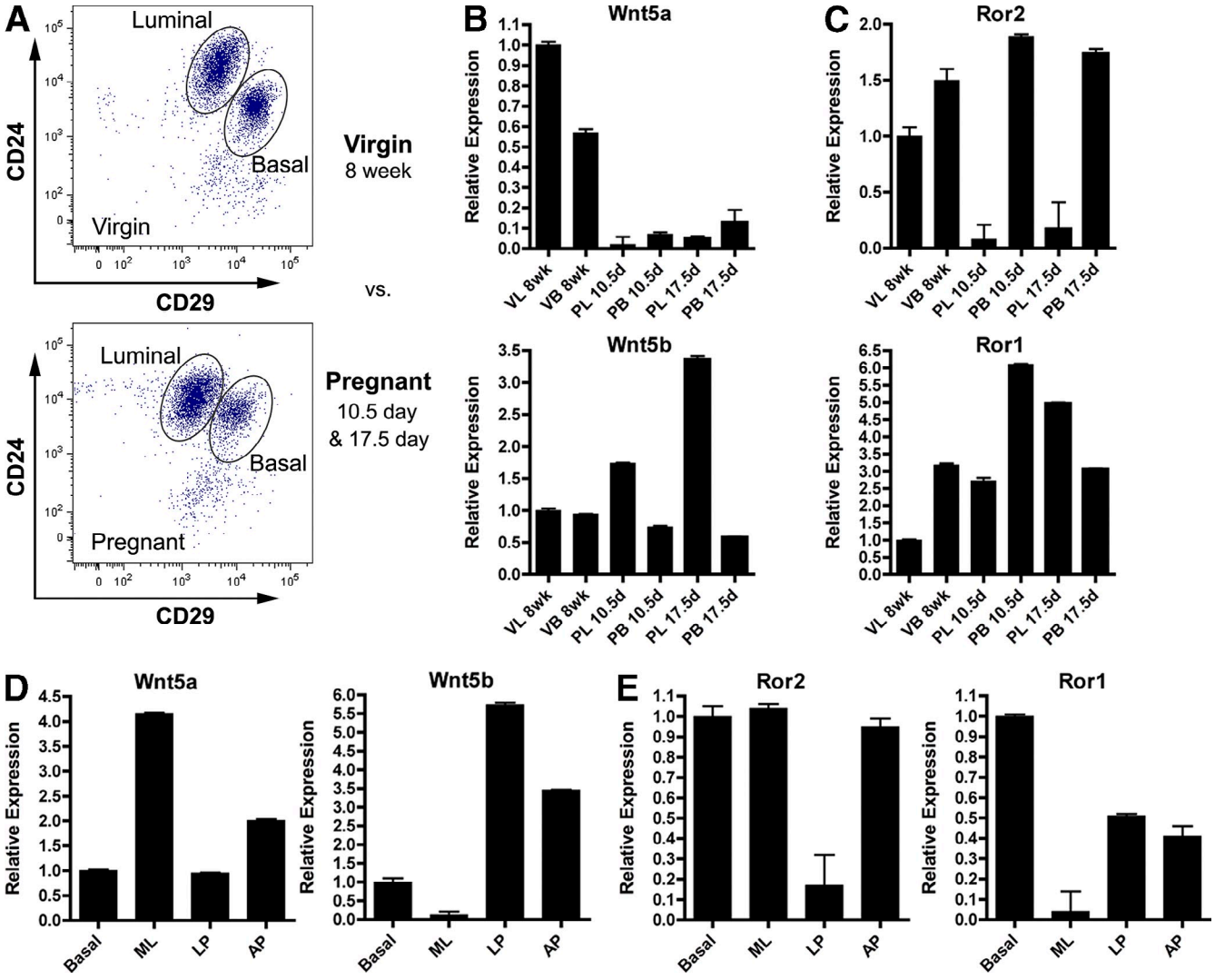

Figure 1. **Ligands and receptors of the Wnt/β-catenin–independent pathway exhibit temporal and spatial regulation in the mammary gland.** (A) Representative FACS plots of luminal ($CD24^+CD29^{lo}$) and basal ($CD24^+CD29^{hi}$) populations from 8-wk virgin and 10.5- or 17.5-d pregnant stages of development. FACS-sorted populations were derived from pools of 15 mice for each stage of development. Scales on the axes represent transformed data for more accurate visual representation of fluorescence units in the lower range of the scale (see Materials and methods for all FACS plots). (B and C) qRT-PCR analysis of the Wnt/β-catenin–independent ligands (B) and receptors (C) within the epithelial compartments (n = 3 replicates for each sorted epithelial fraction). VL, virgin luminal; VB, virgin basal; PL, pregnant luminal; PB, pregnant basal. (D and E) qRT-PCR of Wnt/β-catenin–independent ligands (D) and receptors (E) from luminal populations and basal cells after further refining the luminal population based on CD14 and c-kit from 8-wk-old adult virgin mice. B, basal; ML, mature luminal; LP, luminal progenitor; AP, alveolar progenitor. Plotted values represent means ± SD (error bars).

Wnt/β-catenin signaling activity and Ror2 expression are inversely correlated in the mammary gland

Studies of the Wnt/β-catenin pathway in mammary development have demonstrated its involvement in guiding self-renewal cues and decisions of lineage potential in the mammary epithelium (Zeng and Nusse, 2010; van Amerongen et al., 2012a). Additional reports have shown that Wnt/β-catenin–independent signaling can antagonize the Wnt/β-catenin–dependent pathway (Mikels et al., 2009; Green et al., 2014), yet it remains unclear how these pathways cooperate in vivo where multiple cell types exist under different developmental contexts. We sought to identify the spatial distribution and relationship between Wnt pathways in vivo by probing the location of Wnt/β-catenin activity relative to Ror2 expression in the mammary gland. To analyze Wnt/β-catenin signaling in situ, we used a lentiviral reporter harboring 7TCF/Lef binding sites upstream of *eGFP* (7TCF-*eGFP*; Fuerer and Nusse, 2010) to transduce primary mammary epithelial cells (MECs) and subsequently evaluate Wnt/β-catenin signaling in vivo after transplantation. This reporter reliably identifies Wnt/β-catenin signaling activity in primary MECs in response to both Wnt stimulation and inhibition (Fig. S2, A and B). Significant enrichment of Wnt/β-catenin activity was observed in the TEBs of the developing gland, distinctly localized to the stem-like cap cell layer (Fig. 2, A–C). This activity diminished down the tapered neck of the TEB, where cells differentiate into mature myoepithelial cells (Fig. 2, B and C). An SH2-containing inositol 5′-phosphate (*s-SHIP*; isoform of SH2-containing inositol 5′-phosphatase) promoter controlling *eGFP* expression, previously shown to mark

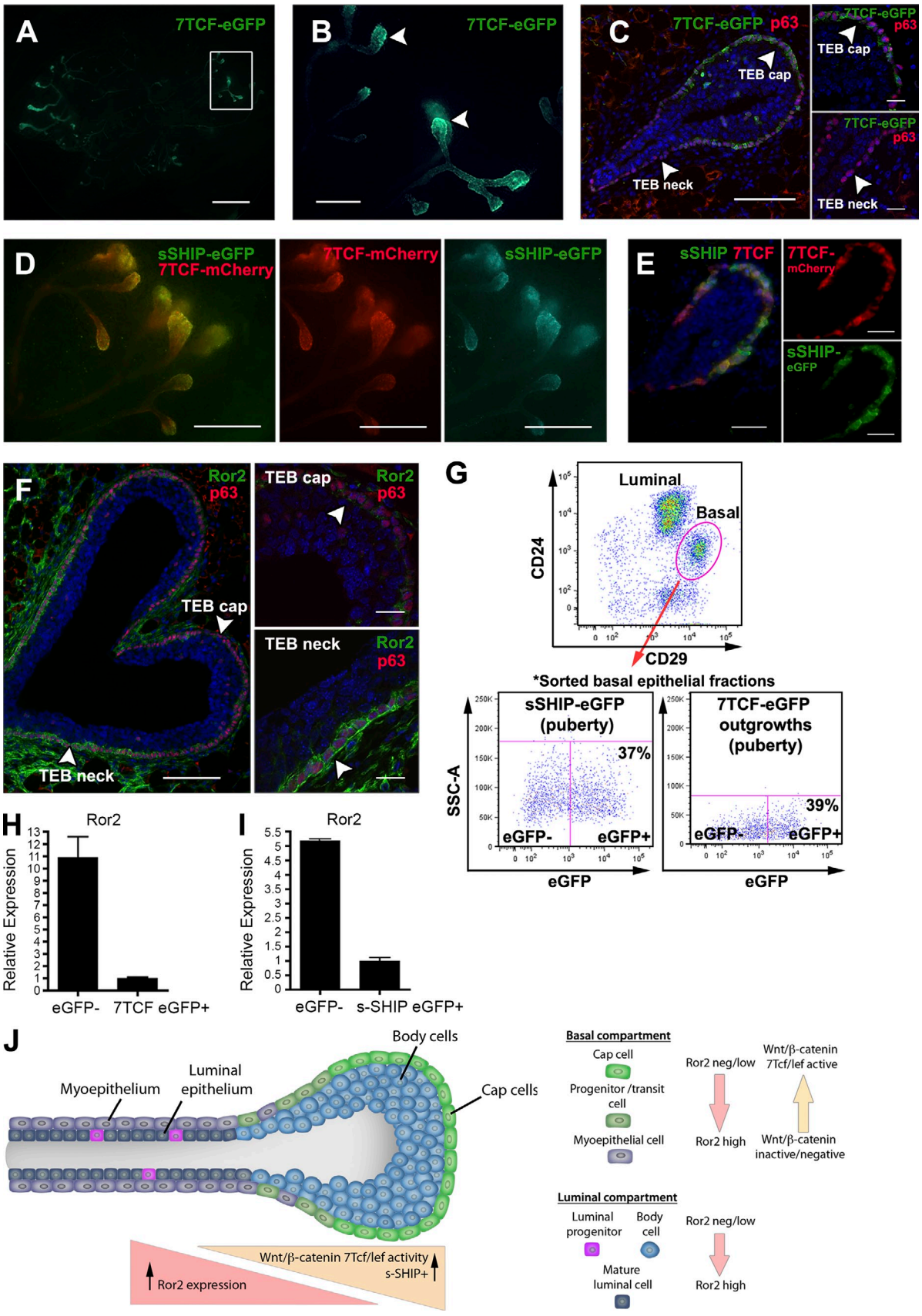

Figure 2. **Wnt/β-catenin signaling activity and Ror2 expression are inversely correlated in the mammary gland.** (A) Fluorescent whole mount of a 4-wk mammary outgrowth harboring a lentiviral *7TCF-eGFP* reporter to survey Wnt activity in vivo. Wnt/β-catenin activity (eGFP) is enriched in the TEBs of the outgrowth (box). (B) Magnification of the boxed region in A of eGFP Wnt/β-catenin TCF activity in the TEBs (arrowheads). (C) IF for eGFP within a

cap cells of the TEB during puberty (Bai and Rohrschneider, 2010), mirrored the expression gradient and localization of Wnt/β-catenin activity in the TEB (Fig. 2, D and E). This overlap of s-SHIP+ cells with Wnt activity was confirmed by evaluating *s-SHIP* outgrowths transduced with a 7TCF/Lef-*mCherry* (7TCF-*mCherry*) Wnt reporter, harboring 7TCF/Lef binding sites upstream of *mCherry*. When the pattern of the alternative receptor Ror2 was examined in the TEB structure, expression was inversely correlated with the location of Wnt/β-catenin activity. Specifically, Ror2 expression was weak in the cap cell layer and gradually more prominent as the cell layers differentiate into mature epithelial layers of the trailing TEB neck and duct (Fig. 2 F). Within the trailing epithelial network, Ror2 was evident in both basal and luminal epithelial layers of the pubertal gland, and this pattern of expression was maintained in the adult virgin ductal network (Fig. S2, C and D).

To provide a more quantitative measure of the inverse expression gradient, *Ror2* levels were evaluated in s-SHIP and 7TCF-*eGFP* models after sorting basal epithelial fractions into GFP+ cap/stem cells versus GFP− bulk basal/myoepithelial cells (Fig. 2 G). Accordingly, in 7TCF-*eGFP* outgrowths, the more committed GFP- basal/myoepithelial cells demonstrated a 10.9-fold higher level of expression of *Ror2* relative to GFP+ cap/stem cells (Fig. 2 H). From the s-SHIP-*eGFP* model, a fivefold higher level of expression of *Ror2* was present in the GFP- basal/myoepithelial cells relative to GFP+ s-SHIP cap/stem cells (Fig. 2 I). Collectively, these data uncover, for the first time in vivo, the inverse relationship of Ror2 expression with Wnt/β-catenin and s-SHIP activity, distinguishing the formation of mature (Ror2-expressing) myoepithelial cells from more primitive (Wnt/β-catenin active) stem cell populations as the mammary gland builds its bilayered epithelial network during puberty (Fig. 2 J).

Wnt/β-catenin–dependent and –independent pathways are integrated in the mammary epithelium

The inverse correlation of Wnt/β-catenin activity with Ror2 expression observed in vivo suggests two conceivable scenarios for how Wnt pathways cooperate in mammary development: (1) Ror2 functions to restrict the localization and intensity of Wnt/β-catenin action by pathway antagonism or (2) distinct Wnt pathways demarcate the differentiation states of the mammary epithelial hierarchy during active morphogenesis. Nevertheless, the assimilation of multiple Wnt inputs in vivo is likely dictated by cell-surface expression of specific Wnt receptors within distinct epithelial populations together with the Wnt ligand combination present within the niche. In light of findings that *Wnt5a* and *Wnt5b* expression patterns were distinct within mammary epithelial subpopulations, the signaling capacities of these Wnts were further interrogated in the mammary epithelium. In an effort to establish which Wnt ligands activate Wnt/β-catenin–dependent versus –independent pathways in MECs, we used an in vitro system of primary MEC monolayer cultures, treating cells with a prototypical Wnt/β-catenin ligand, Wnt3a, alone and in combination with Wnt/β-catenin–independent ligands, Wnt5a and Wnt5b, to assess the interaction of these proteins in the mammary epithelium. The 7TCF-*mCherry* reporter was used as a readout for Wnt/β-catenin–dependent activity. After 24 h, we observed an increase in mCherry-positive cells in response to Wnt3a, whereas Wnt5a and Wnt5b were unable to activate 7TCF-*mCherry* (Fig. 3, A and B). Both Wnt5a and Wnt5b did, however, inhibit the induction of 7TCF-mCherry–positive cells in response to Wnt3a, demonstrating the capacity of both Wnt5a and Wnt5b to antagonize Wnt/β-catenin activity (Fig. 3, A and B). Additionally, qRT-PCR analysis of *Axin2*, a downstream-negative feedback regulator of the Wnt/β-catenin pathway, was used to corroborate the reporter data. After 8 h of Wnt3a treatment, robust *Axin2* mRNA induction was observed (Fig. 3 C). Wnt5a and Wnt5b significantly inhibited Wnt3a-induced *Axin2* expression (Fig. 3 C). The antagonism of Wnt5a and Wnt5b was not a result of receptor competition with Wnt3a, because the phosphorylation of Lrp6 by Wnt3a was equivalently activated in the presence of Wnt5a or Wnt5b (Fig. S3 A). Lentiviral shRNA silencing of *Ror2* abrogated these effects and demonstrated that Ror2 was required to mediate both Wnt5a and Wnt5b inhibition of the Wnt/β-catenin pathway in primary MECs (Fig. 3 D). Interestingly, overexpression of Ror2 in vitro potentiated the ability of Wnt5a, but not Wnt5b, to antagonize Wnt/β-catenin induction in response to Wnt3a (Figs. 3 E and S3 C). This is likely a consequence of sustained Ror2 expression and Wnt5a/Ror2 signaling, as Wnt5a stimulation typically prompts the down-regulation of Ror2 expression in primary MECs (Fig. S3 B). These data not only highlight the integration of Wnt/β-catenin–dependent and –independent pathways in primary MECs, but also reveal an intricate role for Ror2 in conveying Wnt/β-catenin–independent signals elicited by Wnt5a and Wnt5b, offering insight into the coordination of multiple Wnt inputs in vivo.

Ror2 depletion in vivo enhances mammary branching morphogenesis

To identify a role for the Wnt/β-catenin–independent signaling receptor Ror2 in mammary development, a lentiviral shRNA

cross-section of the TEB depicting Wnt/β-catenin activity within the p63+ (red) cap cell layer and minimal in the TEB neck (arrowheads). (D) Fluorescent whole mount of s-SHIP mammary outgrowths transduced with a 7TCF-mCherry reporter depicting overlap within the TEBs (yellow), along with individual channels. (E) IF of sSHIP/7TCF-mCherry TEB section showing overlap of sSHIP-eGFP+ and 7TCF-mCherry+ populations within the cap cells (yellow), along with separate channels. (F) IF for Ror2, demonstrating the increase in Ror2 expression along the neck of the TEB (arrowheads, right) and the limited/absent expression within the cap cell layer (arrowheads, right). (G) Representative FACS plots of the sorting schemes for eGFP+ and eGFP− cells from the basal fractions derived from the s-SHIP model and 7TCF-eGFP outgrowths (n = 9 total glands from s-SHIP model and n = 9 total outgrowths from 7TCF-eGFP transplants, with pools of three glands or outgrowths for each replicate). (H) qRT-PCR demonstrating a 10.9-fold increase in *Ror2* expression in the eGFP− basal/myoepithelial fraction relative to 7TCF-eGFP+ cap/stem cells (n = 3 replicates). (I) qRT-PCR demonstrating a fivefold increase in *Ror2* expression within the eGFP− basal fraction relative to s-SHIP eGFP+ cap cells (n = 3 replicates). Plotted values represent means ± SD (error bars). (J) Model depicting the inverse association of 7TCF/Lef activity and Ror2 expression within the TEB and epithelial subpopulations. Bars: (A) 2 mm; (B) 500 µm; (C, left) 100 µm; (C, right) 20 µm; (D) 1 mm; (E) 50 µm; (F, left) 100 µm; (F, right) 20 µm.

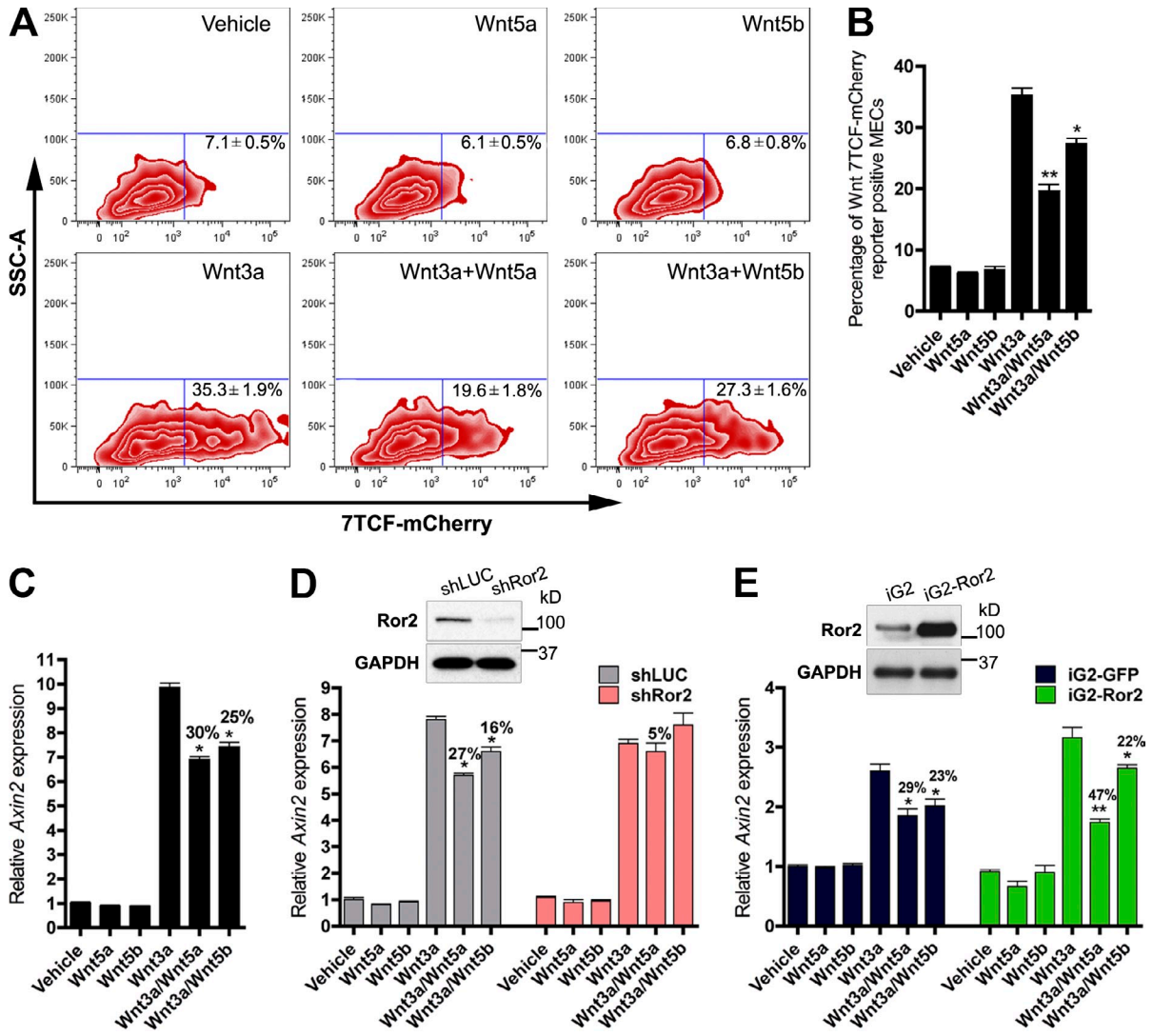

Figure 3. **Wnt/β-catenin–dependent and –independent pathways are integrated in the mammary epithelium.** (A) FACS profiles of primary MECs representing the percentage of 7TCF-mCherry induction after treatment with Wnt3a, Wnt5a, and Wnt5b. Shown are representative FACS plots of three experiments, where treatments were performed in triplicate. (B) Bar graph representing the percentage of Wnt/β-catenin–dependent induction in A by Wnt3a and the degree of inhibition by either Wnt5a or Wnt5b. (C) qRT-PCR analysis of *Axin2* induction after Wnt stimulation. (D) qRT-PCR analysis of *Axin2* after Wnt stimulation in shLUC and shRor2 primary MECs. Depletion of Ror2 expression by shRNA-mediated silencing (illustrated by the Western blot inset) reduced both Wnt5a and Wnt5b antagonism of *Axin2* by Wnt3a. (E) qRT-PCR analysis of *Axin2* in response to Wnt treatments after Ror2 overexpression. Ror2 expression above steady-state levels (illustrated by the Western blot inset) enhanced Wnt/β-catenin pathway repression by Wnt5a (iG2 29% and iG2-Ror2 47% inhibition), but no difference was observed for Wnt5b (iG2 23% and iG2-Ror2 22% inhibition). Plotted values represent means ± SD (error bars). *, $P < 0.05$; **, $P < 0.01$.

strategy was used to silence its expression in vivo. Studies have successfully used this approach for evaluation of gene-specific functions in vivo (Welm et al., 2008; McCaffrey and Macara, 2009; Vafaizadeh et al., 2010; Huo and Macara, 2014). This lentiviral-based system was based on a previously published backbone, LeGO (Weber et al., 2008), together with the U6 promoter/shRNA portion of the pLKO.1 system. Using this system with two independent shRNA hairpins, we achieved 80–90% knockdown of *Ror2* in primary MECs, resulting in efficient silencing of Ror2 protein levels (Fig. 4, A and B).

We transplanted transduced primary MECs into contralateral cleared fat pads of syngeneic hosts to evaluate the developmental outcome of Ror2 depletion in vivo. At 4 wk after transplantation, when TEBs are present, we observed an increase in branching in shRor2 outgrowths relative to contralateral shLUC controls (Fig. 4, C, E, and F). Moreover, shRor2 glands exhibited a 20% decrease in fat pad filling after 4 wk of development, which suggests that increased branching was at the expense of ductal extension (Fig. 4 D). In addition, the TEBs exhibited abnormal morphologies in shRor2 outgrowths relative to proper club-shaped structures that formed in shLUC controls (Fig. 4 G). Around the necks of shRor2 TEBs, where Ror2 expression normally increases, there was a large amount of budding that was not observed in control TEBs (Fig. 4 C, right; and Fig. 4 G). By 8 wk after transplantation, both shLUC and shRor2 mammary outgrowths completed ductal extension and exhibited fully arborized ductal networks; however, an increase in branching persisted in shRor2 glands (Fig. 4, I and J).

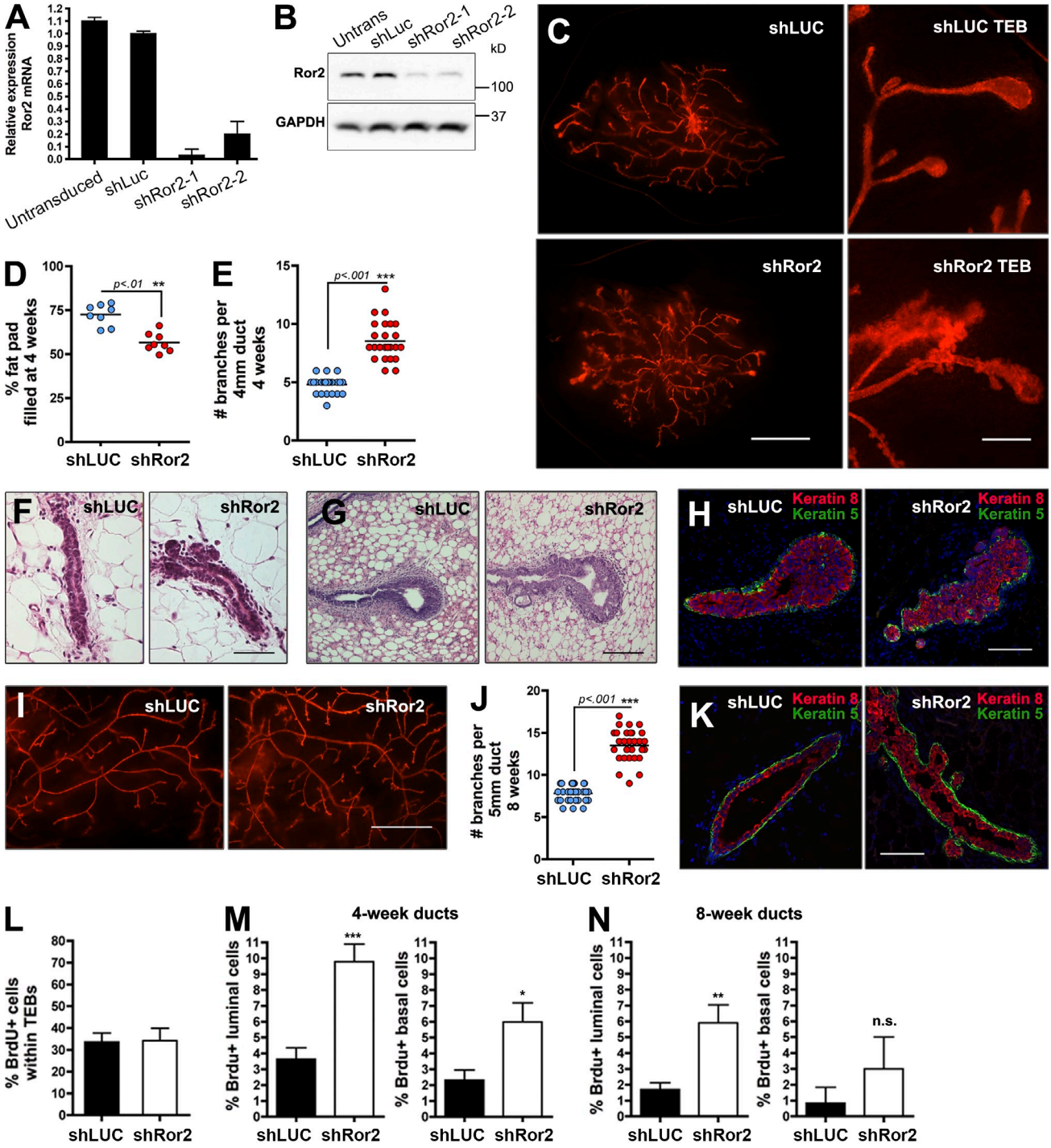

Figure 4. **Ror2 depletion in vivo enhances mammary branching morphogenesis.** (A) qRT-PCR of *Ror2* expression in untransduced, shLUC, and shRor2-transduced primary MECs. Ror2 mRNA knockdown reached ~90% using two independent hairpins. (B) Western blot confirming depletion of Ror2 protein levels in primary MECs. (C) Fluorescent whole mounts of 4-wk shLUC and shRor2 outgrowths after transplantation of lentivirus-infected MECs into contralateral cleared #4 mammary fat pads. Panels on the right depict higher magnification of the TEB structures. (D) shRor2 4-wk outgrowths exhibit a lower percentage of fat-pad-filled relative to shLUC controls (n = 8 contralateral glands). (E) Quantification of the increase in branching morphogenesis in shRor2 outgrowths after 4 wk of development relative to shLUC controls (n = 6 contralateral glands). (F and G) H&E staining of ducts (F) and TEBs (G) from shLUC and shRor2 outgrowths representing the enhanced branching and altered TEB morphology after Ror2 depletion. (H) K8/K5 IF within the TEBs at 4 wk depicting proper luminal (red) and basal (green) epithelial cell compartmentalization in shRor2 outgrowths. (I) Fluorescent whole mounts of 8-wk shLUC and shRor2 outgrowths depicting the increase in branching. (J) Quantitation of the increase in branching morphogenesis in shRor2 outgrowths after 8 wk of development relative to shLUC controls (n = 6 contralateral glands). (K) K8/K5 IF depicting proper luminal (red) and basal (green) epithelial cell compartmentalization in 8-wk outgrowths. (L) Quantification of TEB proliferation, assessed by the percentage of BrdU$^+$ cells. (M) Quantification of ductal BrdU$^+$ cells is shown within 4-wk outgrowths. BrdU$^+$ cells were scored by costaining with the luminal K8 and basal K5 markers (n = 5 contralateral glands). (N) Quantification of ductal BrdU$^+$ cells within 8-wk outgrowths (n = 5 contralateral glands; **, P < 0.01). Bars: (C) 2 mm; (F–H) 50 µm; (I) 2 mm; (K) 50 µm. Plotted values represent means ± SD (error bars). *, P < 0.05; **, P < 0.01; ***, P < 0.001.

Although luminal and basal epithelial layers remained appropriately partitioned in 4- and 8-wk outgrowths as shown by K8 and K5 immunofluorescence (IF; Fig. 4, H and K), proliferative defects were observed. Ror2-depleted TEBs demonstrated levels of proliferation similar to control shLUC TEBs, measured by BrdU incorporation (Fig. 4 L). However, within the subtending ducts of shRor2 4-wk outgrowths, both luminal and basal cells exhibited an increase in proliferation (Fig. 4 M). A slight increase in proliferation remained in 8-wk outgrowths, primarily in the luminal compartment (Fig. 4 N), whereas no differences in apoptosis were observed (Fig. S5 B). Recently, a conditional *Ror2* mouse model was developed (Ho et al., 2012), and using this model, in which the floxed *Ror2* allele was deleted using lentiviral Cre delivery followed by transplantation into the cleared fat pad, we confirmed the shRor2 branching phenotype in vivo (Fig. S4, A and B). A twofold increase in branching was evident after *Ror2* deletion in primary MECs after 8 wk of development, phenocopying shRor2-depleted outgrowths (Fig. S4 C).

Depletion of Ror2 elicits compartment-specific changes in luminal and basal epithelial cell layers accompanied by alterations in the differentiation capacity of the mammary epithelium

Given that Ror2 expression resides in both luminal and basal epithelial compartments, we wanted to determine whether loss of Ror2 elicited changes within these epithelial layers. Luminal and basal epithelial fractions from shLUC and shRor2 outgrowths were evaluated by FACS analysis on the basis of CD24 and CD29 surface marker expression. Of note, the epithelial profile was altered upon Ror2 loss, with a greater proportion of luminal to basal cells in shRor2 outgrowths relative to shLUC controls (Fig. 5, A and B). The LP population, based on CD61, was unchanged in the absence of Ror2 (Fig. S5 A). Given our in vitro observations that Ror2 is required for the inhibition of Wnt/β-catenin–dependent signaling by Wnt5a, we wanted to determine the effects of Ror2 depletion on Wnt activity in vivo. Outgrowths co-transduced with the lentiviral 7TCF–*eGFP* reporter identified appropriate basal localization of Wnt/β-catenin–dependent activity; however, shRor2 outgrowths surprisingly exhibited a decrease in reporter positivity as compared with controls, without any effect on mammosphere-forming ability (Fig. S5, C–E). These data prompted us to seek alternative signaling mechanisms that might dictate the observed shRor2 phenotypes.

Gene expression analysis was subsequently performed on FACS-isolated luminal and basal fractions from shLUC and shRor2 outgrowths to uncover compartment-specific functions for Ror2. Supervised clustering of altered genes revealed eight gene expression groups differentially affected upon Ror2 depletion, corresponding to ∼1,200 altered genes within luminal and basal compartments (Fig. 5 C). Specifically, some gene cohorts exhibited compartment-specific changes (luminal-only vs. basal-only), whereas other genes exhibited alterations in both compartments (with parallel and inverse changes) when Ror2 signaling was silenced. Gene ontology analysis revealed the alteration of genes associated with developmental processes, cell–cell communication, differentiation, actin cytoskeleton organization, and cell adhesion (Fig. 5 D).

The increase in branching observed in shRor2 outgrowths was accompanied by alveolar-like development, which normally occurs during pregnancy. Microarray analysis of the luminal compartment of shRor2 outgrowths revealed the upregulation of genes associated with such differentiation, including *Mal*, *Lalba*, *Csn3*, *Pnck*, and *Clu* (Oakes et al., 2006; Wang et al., 2009). The composition of the luminal epithelial subpopulations determined by c-kit and CD14 was evaluated next, as *Ror2* was differentially expressed in ML, LP, and AP subpopulations (Fig. 1 E). In fact, the luminal epithelial compartment of shRor2 outgrowths contained an increase in APs relative to LPs, whereas shLUC outgrowths contained more LPs relative to APs (Fig. 5, E and F). This AP population was previously defined to exhibit greater milk-forming potential in the absence of a lactogenic stimulus (Asselin-Labat et al., 2011). Changes in the differentiation status of the luminal mammary epithelium were further evaluated in situ. Na-K-Cl cotransporter 1 (NKCC1), a sodium potassium co-transporter present on the basolateral surface of luminal epithelial cells of virgin mammary glands, but lost during pregnancy upon the formation of mature alveoli during differentiation of the mammary ductal tree (Miyoshi et al., 2001), was evaluated by IF. NKCC1 loss was observed in shRor2 outgrowths within areas of high branching and budding (Figs. 5 G and S5 F), which indicates a change in mammary epithelial differentiation. In ∼20% of the shRor2 outgrowths, β-casein expression was detected (Fig. 5 H), further indicating the impact of Ror2 loss on developmental fate. These data, together with our previous observation that *Ror2* expression decreases in the luminal cells during pregnancy, suggest that Ror2 may act to suppress AP expansion and/or differentiation in the luminal compartment before pregnancy. Moreover, the effect of Ror2 loss on differentiation helps explain the loss in luminal expression observed during pregnancy.

Ror2 loss disrupts actin cytoskeletal dynamics during branching morphogenesis

The actin cytoskeleton is an essential component required for coordinated cellular movements during epithelial morphogenesis. In addition to alterations in differentiation capacity of the epithelium upon Ror2 loss, a large cluster of genes associated with actin filament–based processes and the actin cytoskeleton were differentially affected within luminal and basal epithelial compartments (Fig. 6 A). 3D in vitro branching assays were performed to understand the branching defects in shRor2 mammary glands and to characterize the significance of the observed gene expression changes with respect to the actin cytoskeleton. The establishment of 3D branching cultures using primary MECs has provided an instrumental model system with the capability to unravel cellular interactions and coordinated cellular movements required for branching that are difficult to study in vivo (Nelson and Bissell, 2005; Ewald et al., 2008). In this model, branching is initiated by growth factors, such as fibroblast growth factor (FGF) or hepatocyte growth factor (HGF),

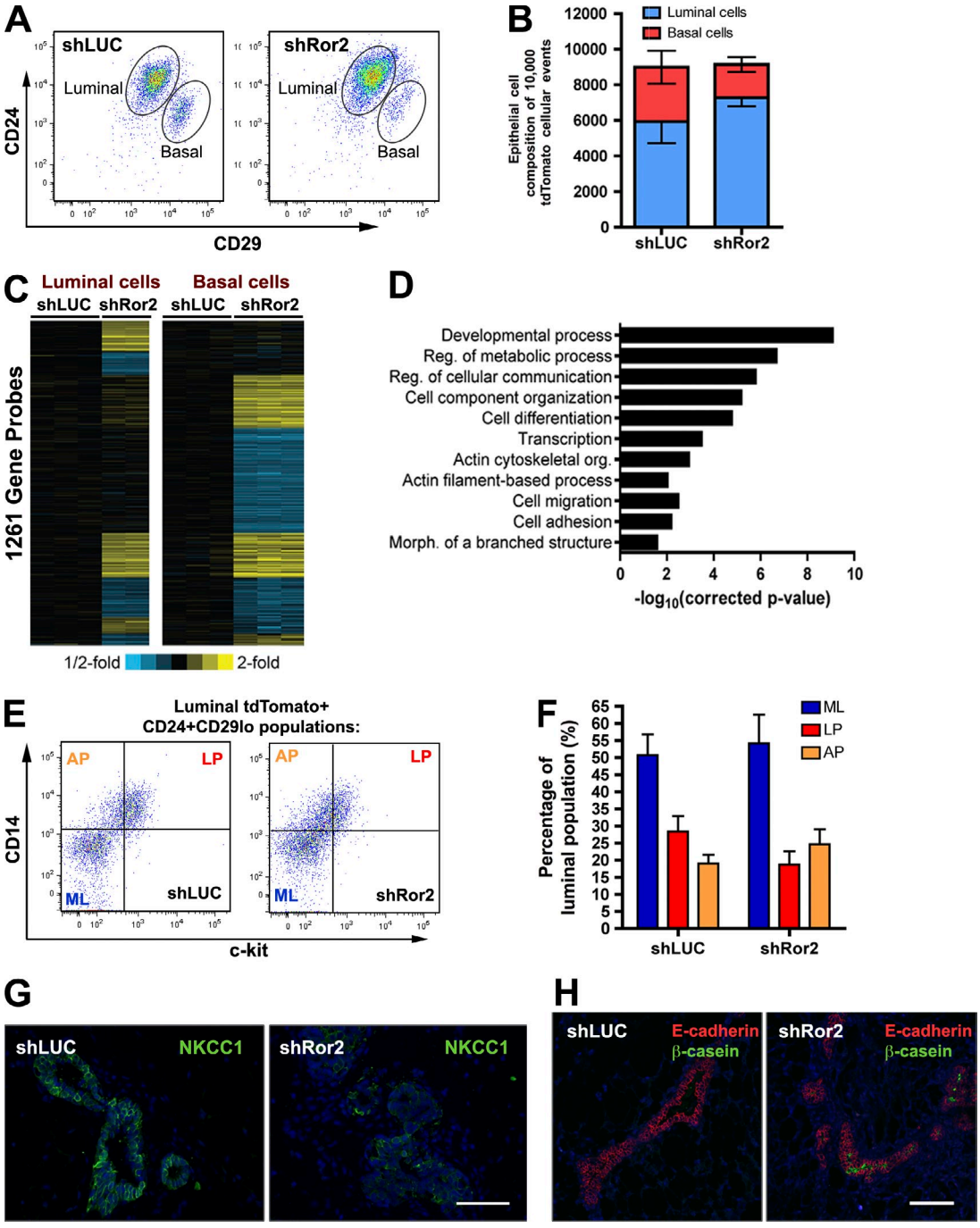

Figure 5. **Depletion of Ror2 elicits compartment-specific changes in luminal and basal epithelial cell layers accompanied by alterations in the differentiation capacity of the mammary epithelium.** (A) CD24/CD29 FACs analysis of tdTomato$^+$ transduced mammary epithelium from shLUC and shRor2 outgrowths at 8 wk depicting luminal and basal epithelial compartments (representative plot of $n = 4$ contralateral shLUC and shRor2 groups). (B) Quantification of the absolute number of luminal and basal epithelial cells from shLUC and shRor2 out of 10,000 tdTomato$^+$ events analyzed ($n = 4$ contralateral groups; shLUC, 5,933 ± 1,219 luminal cells and 3,053 ± 927 basal cells vs. shRor2, 7,278 ± 482 luminal cells and 1,863 ± 1,863 basal cells). (C) Heat map depicting the specific patterns of gene transcript alterations exhibited in luminal and basal epithelial compartments when Ror2 signaling is impaired ($P < 0.01$ and expression changes >1.2 fold). (D) Graphical representation of the gene ontology terms significantly enriched in the shRor2 luminal and basal groups. (E) Representative FACS plots of CD14 and c-kit within the luminal fractions of shLUC and shRor2 groups, depicting ML, AP, and LP fractions (representative plot of $n = 3$ contralateral shLUC and shRor2 groups, each composed of three pooled contralateral pairs from nine mice). (F) Quantitation of ML, AP, and LP fractions within the luminal compartment, showing an increase in AP relative to LP (LP, 18.6 ± 3.9%; AP, 24.7 ± 4.4%) in the shRor2 outgrowths compared with controls (LP, 28.4 ± 4.5%; AP, 19.1 ± 2.5%; $n = 3$, pooled contralateral pairs from nine mice). Plotted values represent means ± SD (error bars). (G) IF for NKCC1, demonstrating loss of NKCC1 staining in shRor2 epithelium compared with the presence of NKCC1 within ducts of shLUC outgrowths. (H) IF for β-casein (green) in shRor2 outgrowths compared with an absence in shLUC controls. E-cadherin staining (red) defines the ducts. Bars, 100 µm.

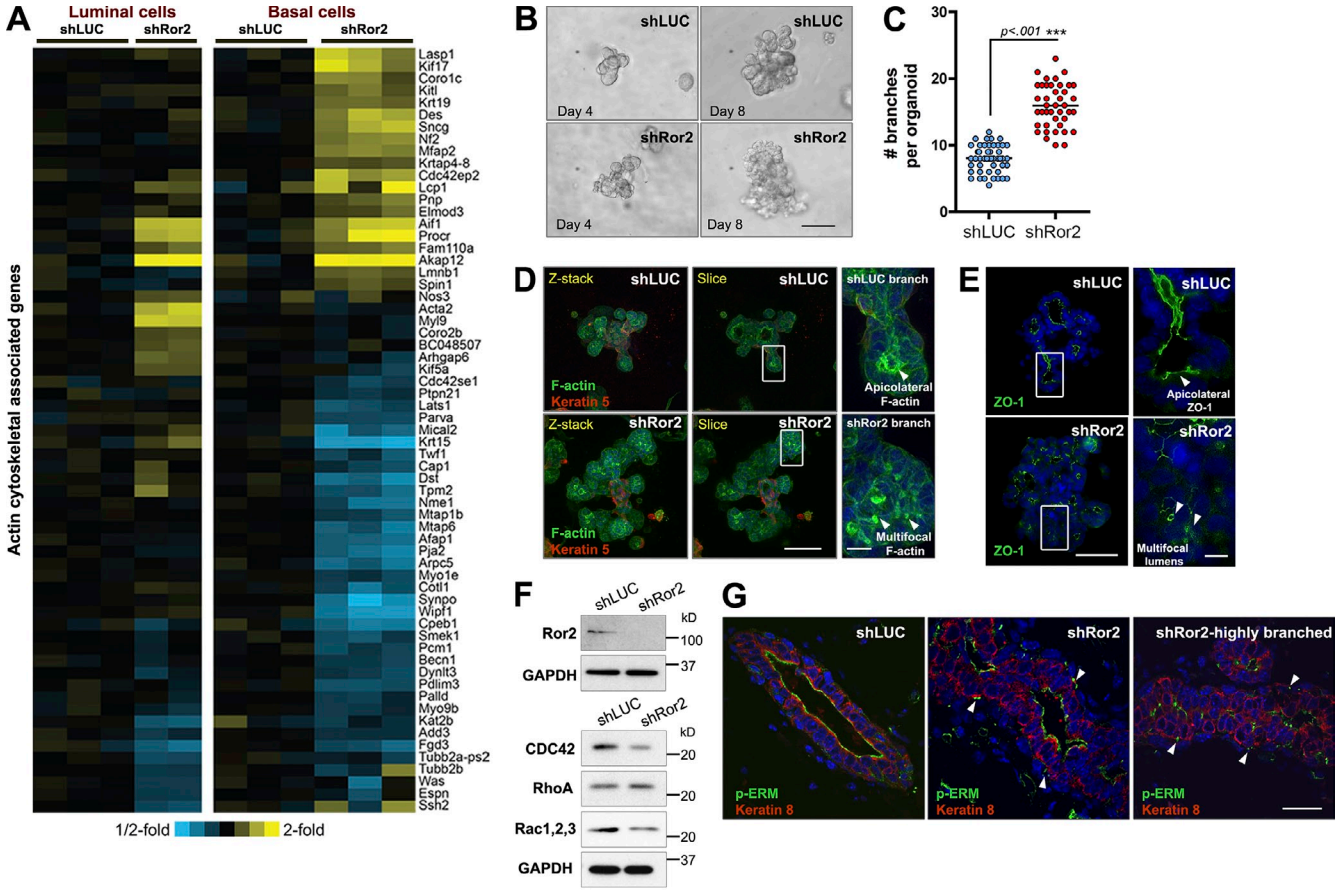

Figure 6. **Ror2 loss disrupts actin cytoskeletal dynamics during branching morphogenesis.** (A) Heat map illustrating the differential alterations in genes associated with actin cytoskeletal dynamics in Ror2-depleted luminal and basal epithelial compartments. (B) Brightfield DIC images of shLUC and shRor2 organoids. Days 4 and 8 are shown to illustrate early and late stages of branching. (C) Quantification of the number of branches emanating from shLUC versus shRor2 organoids (n > 40 organoids per group). (D) Maximum-intensity projections of confocal z stacks and cross-sections depicting F-actin (green) and K5 (red) localization within shLUC and shRor2 organoids. Panels on the right (enlarged from the boxed regions) depict representative areas of F-actin patterns (arrowheads) between shLUC and shRor2 branches. (E) ZO-1 (green) IF depicting microlumens (arrowheads) associated with shRor2 branching organoids. Panels on the right represent magnified representative areas (taken from the boxed regions) of ZO-1 within a branch. (F) Western blot analysis of Rho pathway proteins in shLUC and shRor2 organoids. (G) pERM IF (green) within shLUC and shRor2 ducts. Shown are unbranched and highly branched sections for shRor2 to depict the extremes of the pERM alterations. K8 (red) denotes the luminal cells of the duct. Arrowheads indicate atypical punctate localization of pERM between luminal and basal layers in shRor2 ducts. Bars: (B) 50 µm; (D and E, left) 50 µm; (D and E, right) 8 µm; (G) 25 µm.

and is not dependent on Wnt ligands. Using FGF2-induced branch initiation of transduced mammary epithelium, shRor2 organoids exhibited a twofold increase in branch formation compared with shLUC organoids, recapitulating the in vivo phenotype (Fig. 6, B and C). The excessive branching was also disorganized. Additionally, lentiviral Cre deletion of *Ror2* within $Ror2^{fl/fl}$ organoids phenocopied the increase in branching exhibited by shRor2 organoids compared with Ror2-intact organoids, further validating the lentiviral shRNA model system (Fig. S4, D and E).

Given that many genes associated with actin cytoskeletal dynamics were identified, we subsequently stained shLUC and shRor2 organoids with phalloidin (F-actin) together with the myoepithelial marker K5 (Fig. 6 D). F-actin staining exhibited a multifocal, punctate localization within the branches of shRor2 structures, in contrast to appropriate lateral cell surface and apical positioning along the lumens of shLUC organoids (Fig. 6 D, right panels). Note that, although apical polarization was not compromised in the absence of Ror2, Zona occludens protein 1 (ZO-1), IF revealed the presence of microlumens in multibranched shRor2 organoids (Fig. 6 E, right).

Given the necessity of the Rho family of GTPases in mediating proper actin cytoskeletal dynamics during epithelial morphogenesis (Ewald et al., 2008), we investigated whether Rho pathway alterations were present in response to Ror2 depletion during mammary epithelial branching. Expression of essential mediators of this pathway was investigated at the onset of branching in shLUC versus shRor2 organoids, including cell division cycle 42 (CDC42), Ras homology family member A (RhoA), and RAC1. Interestingly, CDC42 and RAC1 protein levels were reduced as determined by immunoblotting, whereas RhoA protein levels were increased in shRor2 organoids (Fig. 6 F). We next evaluated the in vivo phosphorylation status of the ezrin/radixin/moesin (ERM) family of actin-binding proteins. ERM proteins act downstream of Rho GTPases and have been previously implicated in regulating actin cytoskeleton rearrangements during morphogenesis (Ivetic and Ridley, 2004). Phosphorylated ERM normally localizes to the apicolateral surface

of luminal cells of mammary ducts, as was observed in the ducts of shLUC outgrowths (Fig. 6 G). In ducts and active sites of branching within shRor2 outgrowths, we observed the presence of pERM apically; however, atypical multifocal pERM staining was evident on the basolateral surface of luminal cells in shRor2 ducts, between luminal and myoepithelial cellular compartments (Fig. 6 G). Together, these data provide evidence for Ror2 signaling in regulating proper actin cytoskeleton dynamics, most likely mediated through the Rho pathway and ERM family of proteins to ensure proper luminal/basal epithelial cell integrity and branch formation.

Discussion

In this study, we investigated the role of the alternative Wnt receptor Ror2 in the mammary epithelium and demonstrated a requirement for this receptor in mammary development. First, we established an intricate landscape of Wnt/β-catenin–independent ligand and receptor expression within epithelial subsets of the mammary gland. Moreover, we established the ability of Wnt5a and Wnt5b to antagonize the Wnt/β-catenin pathway in vitro through Ror2 in primary MECs, and discovered the intricate spatial organization exhibited in vivo between the Wnt/β-catenin pathway (Tcf/lef activity) and the Wnt/β-catenin–independent pathway (Ror2 expression). Functional studies revealed a requirement for the Ror2 receptor in orchestrating proper branching morphogenesis and differentiation of the mammary epithelium. These alterations were accompanied by changes in both the luminal and basal epithelium when Ror2 signaling was interrupted. In particular, expression profiling of RNA isolated from luminal and basal epithelial cells from control and shRor2 outgrowths uncovered alterations in genes associated with developmental processes, cell–cell communication, differentiation, actin cytoskeleton organization, and cell adhesion. Lastly, we demonstrated that Ror2 mediates appropriate actin cytoskeletal dynamics during branch formation and provided evidence for the Rho pathway mediating this effect downstream of Ror2.

The expression of multiple Wnt ligands across different stages of mammary development provided early evidence for the involvement of Wnt signaling in these processes (Gavin and McMahon, 1992; Bühler et al., 1993). Subsequent studies extended these observations using in situ hybridization (Kouros-Mehr and Werb, 2006), and, more recently, microarray (Kendrick et al., 2008; Lim et al., 2010) and proteomic (Ji et al., 2011) analyses of sorted epithelial cell fractions. Functional roles for particular Wnt ligands have been previously identified, such as Wnt4 acting downstream of progesterone receptor signaling (Brisken et al., 2000) and Wnt5a downstream of TGF-β signaling (Roarty and Serra, 2007; Pavlovich et al., 2011). More recently, Wnt5a and Wnt5b were established as substrates of MMP3, and Wnt5b was implicated as a negative regulator of mammary stem cell dynamics (Kessenbrock et al., 2013). At present, it remains unclear how the mammary gland assimilates multiple, simultaneous Wnt inputs during development. Recent studies suggest that even a single Wnt protein can elicit diverse signaling activities in vivo depending on the cellular context and combination of receptors present (van Amerongen et al., 2012b). The current study provides significant refinement of the expression patterns of multiple Wnt ligands and receptors in vivo. We identified an intricate pattern of expression shared between *Wnt5a/Ror2* and *Wnt5b/Ror1* within the luminal compartment, which indicates that these Wnt/β-catenin–independent arms of signaling are functioning distinctly in mature versus progenitor subpopulations. Similar trends in ligand/receptor pairs were also observed across developmental stages, highlighting the distinction between *Wnt5a/Ror2* and *Wnt5b/Ror1* signaling in vivo. These findings substantially extend our understanding of the specificity and nonredundant nature of Wnt signaling components within the complex epithelial lineages of the mammary gland. Studies of Wnt5a and Wnt5b function in chondrocytes of the long bones also suggest a distinction among these Wnts in other developmental contexts (Yang et al., 2003).

The cap cell layer of the TEB represents a mammary stem cell reservoir that drives the formation of more mature epithelial lineages of the epithelial bilayer during ductal extension and primary branch formation within puberty (Williams and Daniel, 1983; Srinivasan et al., 2003). We established that the cap cells of the TEB represent an active zone for Wnt/β-catenin activity, and discovered that this activity is inversely correlated with the expression of Ror2, which increases in abundance down the neck of the TEB. We propose a model where Wnt/β-catenin activity provides self-renewal cues for cap/stem cell functionality within the TEB, with Ror2 expression delineating the transition zone where cap and body cells differentiate into more mature epithelial lineages along the basal and luminal hierarchy down the trailing ducts. Within the luminal compartment, Ror2 regulated the composition of ML, AP, and LP populations, where the absence of Ror2 skewed the AP-to-LP pool, altering the differentiation capacity of the mammary epithelium. Within the basal compartment, Ror2 guided the establishment of lineage potential down a more differentiated state. Interestingly, we observed a decrease in expression of genes associated with mesenchymal differentiation (*Trp63*, *Sox9*, *Foxc1*, and *Gja1*) in shRor2 basal cell fractions by microarray profiling. Additionally, *Procr*, a newly identified multipotent mammary stem cell marker (Wang et al., 2014), was elevated in the microarray within shRor2 basal fractions, which suggests that progression of a basal stem/progenitor cell to a more differentiated myoepithelial cell requires Ror2 signaling. These data further suggest a scenario where the Wnt receptor dictates, at least in part, the developmental outcome of the mammary epithelium. Wnt signal specificity and heterogeneity within the mammary gland are likely not determined solely by the receptor context, given that multiple Wnt ligands, receptors, coreceptors, and downstream signaling players exist. Local Wnts that supply spatial cues to orient the plane of division and determine cell fate within the TEB could potentially represent another aspect of guidance provided by Wnt signaling during active morphogenesis and lineage commitment, as has been demonstrated with embryonic stem cells in vitro (Habib et al., 2013). Moreover, signaling gradients specified by individual Wnt ligands, or other extracellular Wnt modulators, could provide an additional level of Wnt signaling refinement during mammary development (Kiecker and Niehrs, 2001; Harterink et al., 2011).

Reciprocal relationships between Wnt/β-catenin–dependent and –independent signaling, with regard to self-renewal and differentiation processes, have been observed in other models of development, regeneration, and aging (Green et al., 2007, 2008; Stoick-Cooper et al., 2007; Florian et al., 2013). In some cellular contexts, Wnt/β-catenin–dependent pathway antagonism by Wnt/β-catenin–independent mechanisms exist in several cell types and within certain tissues, mediated predominantly by Wnt5a. Multiple studies have demonstrated that this antagonism is elicited through the tyrosine kinase activity of Ror2 (Mikels and Nusse, 2006; Mikels et al., 2009), although other mechanisms have been observed (Grumolato et al., 2010). In our studies, both Wnt5a and Wnt5b antagonized Wnt/β-catenin–dependent activity in primary MECs, whereas disruption of Ror2 expression in vitro abrogated these effects. Ror2 overexpression, however, potentiated the antagonism of Wnt/β-catenin activity in MECs; however, this effect was specific only for Wnt5a. These data suggest that the mechanism of inhibition by Wnt5b likely does not depend on Ror2 abundance, but on that of another receptor, perhaps Ror1. Given that Lrp6 activation was maintained in Wnt3a-treated cultures with either Wnt5a or Wnt5b, the mechanism of antagonism is likely a result of downstream signaling elicited by Wnt/β-catenin–independent signaling, including the Ca^{2+}/CamKII→PKC→NFAT pathway (Angers and Moon, 2009). The decrease in abundance of the 7TCF-*eGFP* reporter in vivo in response to Ror2 depletion was surprising based on our in vitro data. We propose two explanations for these observations. First, Ror2 loss prompted the down-regulation of genes associated with mesenchymal differentiation, which could alter integrity of the bulk basal/myoepithelial cell population, and thus indirectly affect Wnt/β-catenin–responsive stem cells. No differences in primary or secondary mammosphere formation between basal FACS-sorted cells from shLUC and shRor2 outgrowths were observed, which suggests that myoepithelial differentiation rather than self-renewal was compromised. Second, in vitro assays involve a defined interaction of multiple Wnts and short-term responses that are not necessarily reflected in vivo, where multiple Wnt pathway modulators and additional Wnt ligand and receptor interactions between multiple cell types are likely occurring. For instance, Ror2 interactions with Fzd have been demonstrated in other cellular contexts, distinguishing Wnt/β-catenin–dependent versus –independent signaling decisions when Fzd couples to either Ror2 or Lrp5/6 (Grumolato et al., 2010; Nishita et al., 2010). Alternatively, in *C. elegans*, the Ror homologue, Cam-1, exhibits a non–cell-autonomous mechanism of Wnt pathway antagonism by means of sequestering Wnts and fine-tuning the pattern of Wnt pathway activity and cellular fate (Green et al., 2007). Additionally, the potential for Wnt gradient influences on specifying the Wnt signaling output, together with the possibility of unique Wnt–Wnt interactions in vivo, presents another layer of complexity that needs to be explored further in the mammary gland (Cha et al., 2008; Nalesso et al., 2011). Therefore, our results highlight the intricacy of Wnt pathway components in vivo and the potential of Ror2 to engage additional Wnt ligands, receptor interactions, and other modulators of the pathway.

How cells actively collaborate and communicate during the shaping of an organized epithelial structure such as the mammary gland remains an evolving puzzle. Alternative Wnt/β-catenin–independent pathways are instrumental in guiding embryonic development by providing the instructive cues essential for tissue morphogenesis and by dictating appropriate cellular movements in concert with proper orientation of cells within a particular plane of a tissue. Roles for Wnt/β-catenin–independent signaling in planar cell polarity and convergent extension movements, spanning *Drosophila melanogaster*, *Xenopus laevis*, zebrafish, and mammalian models, highlight their critical function in directing morphogenesis (van Amerongen, 2012). For instance, in the developing mouse embryo, Wnt/β-catenin–independent pathways serve an essential function in coordinating development of several organs, including the skeleton, heart, and nervous system (Yamaguchi et al., 1999; DeChiara et al., 2000; Takeuchi et al., 2000; Ho et al., 2012). In the mammary gland, branching morphogenesis is a key developmental process required for proper patterning of the epithelium, yet the regulatory mechanisms guiding appropriate tissue architecture are still incomplete (Gjorevski and Nelson, 2011). Elegant in vitro models have helped define the cellular cooperation that takes place during branching morphogenesis of the mammary epithelium, as well as some of the factors that govern these processes. One such pathway implicated in proper epithelial morphogenesis during branching is the Rho pathway, responsible for coordinating the collective movement of epithelial cells. Essential components of this pathway, including CDC42, Rho, Rac1, and ROCK, have been implicated in mediating appropriate branch formation during active epithelial morphogenesis, specifically coordinating both branch initiation and extension (Ewald et al., 2008; Bray et al., 2011; Zhu and Nelson, 2013). Our discovery that protein expression levels of multiple Rho pathway components were altered in Ror2-depleted organoids during active branching morphogenesis in 3D cultures demonstrates the imbalance of Rho signaling imparted by Ror2 depletion. The net biological effect of these signaling alterations in the mammary epithelium was inappropriate branching morphogenesis, accompanied by mislocalized intercellular F-actin within shRor2 branches in vitro and improper positioning of phosphorylated ERM within the epithelial bilayer of shRor2 ducts in vivo. The current study, therefore, assigns the Wnt/β-catenin–independent receptor Ror2 as an important regulator of proper branching through the regulation of actin cytoskeleton dynamics during epithelial morphogenesis. Intriguingly, given the inverse relationship of Ror2 expression with the Wnt/β-catenin pathway in more mature versus primitive epithelial populations within the mammary gland, the establishment of lineage commitment down a more differentiated path could be related to actin cytoskeletal cues mediating cell fate decisions, as has been observed in epidermal stem cells (Connelly et al., 2010). The precise mechanisms downstream of Ror2 that signal to regulate the Rho pathway remain to be elucidated.

This study establishes the coordinated regulation of Wnt/β-catenin–dependent and –independent pathways in the context of postnatal mammary gland development and assigns a role for Ror2 in the regulation of proper branching and differentiation

in vivo. In-depth characterization of Wnt signaling interactions in mammary development is a necessary prerequisite for understanding the cooperation of Wnt signaling pathways in heterogeneous cell populations within breast cancers (Cleary et al., 2014). Given the association of the Wnt/β-catenin–dependent pathway with basal-like breast cancers (DiMeo et al., 2009; Khramtsov et al., 2010), further characterization of Wnt specificity and Wnt pathway integration in the context of tumorigenesis is warranted. Future studies should yield significant insight into the role of Wnt-β-catenin–dependent and –independent signaling in the regulation of tumor heterogeneity and cellular interactions during cancer progression.

Materials and methods

Mouse strains and maintenance

This study was performed in accordance with the rules of the Guide for the Care and Use of Laboratory Animals of the National Institutes of Health. All mice were maintained and euthanized according to the guidelines of the Institutional Animal Care and Use Committee of Baylor College of Medicine under the approved protocol AN-504. FVB/NJ and Ror2$^{fl/fl}$ mice were purchased from Jackson ImmunoResearch Laboratories. The Ror2 conditional allele was generated by flanking exons 3 and 4 with lox2272 sites (Ho et al., 2012). The s-SHIP transgenic mouse model was provided by L. Bai (from the laboratory of L. Rohrschneider, Fred Hutchinson Cancer Research Center, Seattle, WA).

Lentiviral plasmids

Lentiviral shRNA sequences were derived from the pLKO.1 library purchased from GE Healthcare. The lentiviral backbone Lentiviral Gene Ontology Vector (LeGO-T) was provided by K. Riecken (University Medical Center Hamburg, Hamburg, Germany; now deposited in Addgene). The U6 promoter with shRNA hairpins from pLKO.1 were PCR amplified with the addition of restriction sites Xba1 and Not1, and cloned into LeGO-T harboring a constitutive tdTomato fluorescent marker downstream of a Spleen Focus Forming Viral Promoter (SFFV). The shRNA antisense sequences were as follows: shLUC, 5′-ATTCCAATTCAGCGGGGGC-3′; shRor2-1, 5′-TATTCTGCGTAAAGCACCACG-3′; and shRor2-2, 5′-ATGAGTTTGTAGTAATCTGCG-3′. Clones were sequence validated and digested to ensure proper insertion of each U6-shRor2 hairpin into LeGO-T. Five hairpins against Ror2 were cloned. LeGO-iG2 was used for Ror2 overexpression studies.

Primary MEC isolation

Primary MECs were isolated as described previously (Shore et al., 2012). The third, fourth, and fifth mammary glands were harvested from virgin or pregnant stages of development. In the case of transplants, the fourth pair was used. Glands were subsequently weighed and manually minced into 1 mm × 1 mm fragments between two scalpels. Mammary organoids were derived by digesting the glands in DMEM/F12 containing 1 mg/ml Collagenase A (Roche) for 2 h at 37°C with constant rotation at 125 rpm. The digest was subjected to differential centrifugation to enrich for organoids by performing a series of short centrifugation steps (8 s at 1,500 rpm, performed three to four times). The enriched epithelial organoid preparation was subjected to 0.25% trypsin at 37°C for 5 min, washed, and filtered through a 0.40-µm cell strainer to obtain single MECs. Single cells were washed twice with PBS before transduction, RNA isolation, or FACS staining.

Lentiviral transduction of primary MECs

Transduction of primary MECs was performed as described previously (Welm et al., 2008), with modifications. Single MECs were seeded at a density of 500,000–1,000,000 cells in a 24-well low-attachment plate and infected at an MOI of 30 with designated lentivirus in 800 µl of growth media. Growth media was defined as DMEM/F-12 supplemented with 10% FBS, 5 µg/ml insulin, 10 ng/ml mouse EGF, and 1 µg/ml hydrocortisone. Cells were infected overnight for ∼16 h. The following day, aggregated cells were washed three times with PBS and resuspended in a 1:1 ratio of growth factor–reduced Matrigel/HBSS at 100,000 cells per 10 µl volume for injection. For 7TCF in vitro reporter experiments in primary MECs, transduced cells were plated in monolayers and treated with Wnt3a (40 ng/ml), Wnt5a (100 ng/ml), Wnt5b (100 ng/ml), and DKK1 (100 ng/ml) alone and in combination.

FACS staining and analysis

Lineage-positive cells were depleted from the cell preparation using the EasySep Mouse Mammary Stem Cell Enrichment kit (catalogue no. 19757; Stemcell Technologies). For transduced epithelial populations, tdTomato fluorescence was used to positively select Lin$^-$ MECs for analysis and sorting. Single cell preparations were resuspended at a concentration of 10^7 cells/ml in HBSS$^+$ (containing 2% FBS with 10 mM Hepes buffer) for antibody staining. All antibody incubations were performed on ice for 30 min. Cells were stained with anti–mouse CD24-Pacific Blue (1:100; BioLegend) and anti–mouse CD29-APC (1:100; BioLegend) to separate the luminal and basal epithelial fractions. LP fractions were isolated by segregating the luminal CD24$^+$CD29^{lo} fraction based on either (1) CD61 or (2) the combination of CD14 and c-kit, as described previously (Shore et al., 2012). FACS staining of the LPs was performed with anti–mouse CD61-FITC (1:100; BioLegend), anti–mouse CD117(c-kit)-PE (Clone ACK4, 1:50; Cedarlane Laboratories), anti–mouse CD117(c-kit)-APC (Clone 2B8, 1:50; BD), and anti–mouse CD14-FITC (1:50; eBiosciences). For analysis of LPs from tdTomato$^+$ shLUC and shRor2 outgrowths, the APC-conjugated CD117 was used in place of the PE-conjugated CD117 and anti–mouse CD24-APC-Cy7 (1:100; BioLegend) was used in place of CD24-PacBlue. Cells were either FACS analyzed using a cell analyzer (LSR Fortessa; BD) or FACS sorted using a cell sorter (Aria II; BD). Processing of FACS data was performed using FlowJo, version 9.5.3 (Tree Star). All FACS plots depict compensated data that has been display transformed, where the scale is compressed in the lower range of the axes, leading to more accurate visual representation of fluorescence units in the lower range of the scale (http://www.flowjo.com/v76/en/displaytransformwhy.html; Herzenberg et al., 2006).

RNA isolation and gene expression profiling

RNA from sorted mammary cell populations was isolated using TRIzol reagent (Life Technologies). RNA from sorted shLUC and shRor2 samples was isolated using the Arcturus PicoPure kit (KIT0204) from Applied Biosystems. The Baylor College of Medicine Genomic and RNA Profiling Core (GARP) performed sample quality checks using the ND-1000 (Nanodrop) and a Bioanalyzer Nano chip (Agilent Technologies). RNA was amplified from biological triplicates using NuGEN Ovation Pico WTA V2 kit (catalogue no. 3302-12) and Cy3-labeled using the Agilent Quick Amp Labeling kit (for one color) protocol version 6.5. The Baylor College of Medicine GARP Core performed hybridizations of the labeled product to Agilent Sure Print 3 Mouse GE 8 × 60,000 microarrays. Array data were deposited in the Gene Expression Omnibus (accession no. GSE57985). Arrays were processed and quantile normalized using Bioconductor, and the identification of genes significant in either basal or luminal populations between shLUC and shRor2 was determined by a *t* test ($P < 0.01$, log-transformed data, two-sided) and fold change >1.2 in either direction. Expression values were centered on the mean of the corresponding shLUC control group, and genes were clustered using a previously described approach (Creighton et al., 2008): (1) each pattern of interest was represented as a series of 1 s, 0 s, and 21 s; (2) for each gene, the Pearson's correlation was computed between its expression values and each of the predefined patterns; (3) the pattern best correlated with the expression of each gene was determined, and the genes were manually sorted based on their assigned patterns. Color maps were rendered using Java TreeView (Saldanha, 2004).

Quantitative RT-PCR

qPCR was performed using SYBR green methodology (Applied Biosystems). Primer sequences (listed in Table S1) were designed using the Roche Universal Probe Library. Relative gene expression changes were determined after normalizing to β-actin and calculating the ΔΔCT. SD calculations were performed on the fold changes observed among the biological replicates, derived from the calculated $2^{-\Delta\Delta Ct}$.

Mammary gland processing and immunostaining

For proliferation analysis, mice were administered 60 µg/gram body weight BrdU via IP injection 2 h before sacrifice. Fluorescent whole-mount analysis of mammary branching was performed on paired contralateral outgrowths of the same mouse. Fluorescent whole-mount images were acquired by sandwiching glands between two glass slides and imaging on a stereomicroscope (Leica). Glands were fixed in 4% paraformaldehyde overnight at 4°C before processing to paraffin blocks. For immunostaining,

sections were deparaffinized, rehydrated, and subjected to Tris-EDTA (10 mM Tris Base, 1 mM EDTA solution, and 0.05% Tween 20, pH 9.0) antigen retrieval for 20 min in a microwave. Primary antibody incubations were performed overnight at 4°C. Antibodies and concentrations were as follows: mouse anti-Ror2 (1:100; Nt 2535-2835, Ror2-s; Developmental Studies Hybridoma Bank), mouse anti-EGFP (1:250; JL-8, 632381; Living Colors), rat anti-K8 (1:250; TROMA-1; Developmental Studies Hybridoma Bank), rabbit anti-K5 (1:5,000; PRB-160P; Covance), rabbit anti-p63 (1:200, ΔN-p63, 619002; BioLegend), rat anti-BrdU (1:250; ab6326; Abcam), rabbit anti-CC3 (1:200; 9661; Cell Signaling Technology), rabbit anti-NKCC1 (1:1,000; supplied by J. Turner, National Institutes of Health, Bethesda, MD), mouse anti–β-casein (1:300; supplied by M. Bissell, University of California, Berkeley, Berkeley, CA), and rabbit anti-pERM (1:500; Cell Signaling Technology). For Ror2 IF, tyramide signal amplification was performed according to the instructions for the TSA Fluorescein System (NEL701A001KT; PerkinElmer).

In vitro mammary branching assays

Primary MECs were transduced overnight in suspension culture as described earlier. The following day, 8-well chamber slides were coated with a thin layer of growth factor–reduced Matrigel (5 µl). In brief, aggregated organoids from the overnight transduction were washed twice in PBS before suspending in ice-cold growth factor–reduced Matrigel at a density of 100,000 cells per 40 µl. Within each coated chamber, 40 µl of the cell suspension was plated and allowed to solidify at 37°C for 30 min. The resultant embedded cultures were overlaid with 500 µl of basal medium (1 × insulin/transferrin/selenium [ITS], 1 × penicillin/streptomycin [PS] in DMEM/F12) supplemented with 2.5 nM FGF2 for the induction of branching morphogenesis.

Mammosphere assay

FACS-sorted basal fractions from 8-wk shLUC and shRor2 outgrowths were resuspended in mammosphere media and seeded at a density of 5,000 cells per well in a low-attachment 12-well plate. Primary mammospheres were scored after 7 d. Secondary spheres were generated by dissociating primary spheres with 0.05% Trypsin and mechanical means, filtering the resulting suspension through a 40-µm cell strainer, and then plating 2,000 cells per well from shLUC and shRor2 groups in a low-attachment 12-well plate. Secondary spheres were scored after 7 d. Mammosphere media was composed of DMEM/F12 with 20 ng/ml bFGF, 20 ng/ml EGF, and B27 supplement.

Microscope image acquisition

All stained samples were mounted in Aqua Poly/Mount imaging medium (18606; Polysciences Inc.), and microscopy was performed at room temperature. Confocal images were acquired using a confocal laser scanning microscope (Nikon A1R-s; four PMTs plus white light detector) equipped with Elements acquisition software (Nikon). 60× Plan-Apochromat/1.4 NA oil objective and 100× Plan-Apochromat/1.4 NA oil objective lenses were used. For general epifluorescence, images were captured with a microscope (BX-50; Olympus) with a SPOT CCD camera (SPOT 7.4 Slider RTKE; Diagnostic Instruments) and SPOT Advanced software. On the BX-50 microscope, 20× U-Plan-Apochromat/0.70 NA and 40× U-Plan-Apochromat/0.85 NA objective lenses were used. For fluorescent whole mounts, images were acquired with a microscope (Leica MZ16F; optical zoom 0.71×–5×) with a digital color camera (DFC300FX; Leica) and Image Pro Plus 6.1 software (Media Cybernetics). An Axio Observer.A1 microscope (Carl Zeiss) was used for differential interference contrast (DIC) image capture, with 10× A-Plan/0.25 NA Ph1 and 20× LD-Plan/0.4 NA Ph2 Korr objective lenses. A camera (AxioCam MRm; Carl Zeiss) and digital image acquisition software (AxioVision) were used for DIC images. Fluorochromes included Alexa Fluor 488, Alexa Fluor 594, and Fluorescein. All nuclei were detected by DAPI staining. Photoshop CS3 (Adobe) was used when necessary to adjust levels within each channel equally across all images to maximize image clarity.

Statistical analysis

Unpaired Student's *t* tests were performed on analyses involving two-group comparisons, with the exception of mammary branching and percent fat-pad-filled calculations. Mammary branching and percent fat-pad-filled quantitation were performed on contralateral shLUC and shRor2 glands of the same mice using a paired Student's *t* test. One-way ANOVA followed by a Tukey post-test was performed on experiments involving three or more groups. All quantitative measurements were performed in ImageJ or Excel (Microsoft; *, $P < 0.05$; **, $P < 0.01$; ***, $P < 0.001$). Plotted values represent means ± SD.

Online supplemental material

Fig. S1 contains the sort validation and analysis of additional Wnt ligands within sorted epithelial cells from virgin and pregnant stages of development. Fig. S2 demonstrates the validation of *7TCF-eGFP* in primary MECS and also includes Ror2 IF staining within the ducts of 6 wk and 8 wk glands. Fig. S3 illustrates additional signaling outcomes in primary MECs after Wnt stimulation, relating to Lrp6 and Ror2. Fig. S4 depicts the lentiviral-Cre approach for deleting Ror2 in primary $Ror2^{fl/fl}$ MECs, used to validate the in vivo phenotypes displayed by shRNA depletion. Fig. S5 contains additional phenotypic analysis of shLUC and shRor2 outgrowths, including CD61 progenitor analysis, apoptosis evaluation, FACS analysis of Wnt activity in vivo from shLUC and shRor2 outgrowths, mammosphere forming capacity, and NKCC1 staining within shLUC and shRor2 TEBs. Table S1 includes all qRT-PCR primer sequences. Online supplemental material is available at http://www.jcb.org/cgi/content/full/jcb.201408058/DC1. Additional data are available in the JCB DataViewer at http://dx.doi.org/10.1083/jcb.201408058.dv.

This work was conducted with the help of the Baylor College of Medicine Cytometry and Cell Sorting Core (National Institutes of Health [NIH] P30 AI036211, P30 CA125123, and S10 RR024574), the Genomics and RNA Profiling Core, the Integrated Microscopy Core (NIH HD007495, DK56338, and CA125123), the Dan L. Duncan Cancer Center, the John S. Dunn Gulf Coast Consortium for Chemical Genomics, and the Lester and Sue Smith Breast Center Pathology Core. We would like to thank Dr. Kristoffer Reicken for the LeGO vectors and Lixia Bai from the laboratory of the late Dr. Larry Rohrschneider for the s-SHIP mice. Special thanks to Dr. Emily Roarty, Dr. Amy Shore, and Amulya Sreekumar for critical reading of the manuscript.

This work was funded by a National Cancer Institute Award NCI R01 CA016303-38 to J.M. Rosen and by a Department of Defense Postdoctoral Fellowship Award W81XWH-10-1-0356 to K. Roarty.

The authors declare no competing financial interests.

Author contributions: K. Roarty and J.M. Rosen conceived and designed the experiments. K. Roarty and A.N. Shore performed the experiments. K. Roarty, A.N. Shore, C.J. Creighton, and J.M. Rosen analyzed the data. K. Roarty and J.M. Rosen wrote the manuscript.

Submitted: 12 August 2014
Accepted: 16 December 2014

References

Angers, S., and R.T. Moon. 2009. Proximal events in Wnt signal transduction. *Nat. Rev. Mol. Cell Biol.* 10:468–477.

Asselin-Labat, M.L., K.D. Sutherland, F. Vaillant, D.E. Gyorki, D. Wu, S. Holroyd, K. Breslin, T. Ward, W. Shi, M.L. Bath, et al. 2011. Gata-3 negatively regulates the tumor-initiating capacity of mammary luminal progenitor cells and targets the putative tumor suppressor caspase-14. *Mol. Cell. Biol.* 31:4609–4622. http://dx.doi.org/10.1128/MCB.05766-11

Badders, N.M., S. Goel, R.J. Clark, K.S. Klos, S. Kim, A. Bafico, C. Lindvall, B.O. Williams, and C.M. Alexander. 2009. The Wnt receptor, Lrp5, is expressed by mouse mammary stem cells and is required to maintain the basal lineage. *PLoS ONE*. 4:e6594. http://dx.doi.org/10.1371/journal.pone.0006594

Bai, L., and L.R. Rohrschneider. 2010. s-SHIP promoter expression marks activated stem cells in developing mouse mammary tissue. *Genes Dev.* 24:1882–1892. http://dx.doi.org/10.1101/gad.1932810

Bray, K., C. Brakebusch, and T. Vargo-Gogola. 2011. The Rho GTPase Cdc42 is required for primary mammary epithelial cell morphogenesis in vitro. *Small GTPases*. 2:247–258. http://dx.doi.org/10.4161/sgtp.2.5.18163

Brisken, C., A. Heineman, T. Chavarria, B. Elenbaas, J. Tan, S.K. Dey, J.A. McMahon, A.P. McMahon, and R.A. Weinberg. 2000. Essential function of Wnt-4 in mammary gland development downstream of progesterone signaling. *Genes Dev.* 14:650–654.

Bühler, T.A., T.C. Dale, C. Kieback, R.C. Humphreys, and J.M. Rosen. 1993. Localization and quantification of Wnt-2 gene expression in mouse mammary development. *Dev. Biol.* 155:87–96. http://dx.doi.org/10.1006/dbio.1993.1009

Cha, S.W., E. Tadjuidje, Q. Tao, C. Wylie, and J. Heasman. 2008. Wnt5a and Wnt11 interact in a maternal Dkk1-regulated fashion to activate both canonical and non-canonical signaling in *Xenopus* axis formation. *Development*. 135:3719–3729. http://dx.doi.org/10.1242/dev.029025

Chu, E.Y., J. Hens, T. Andl, A. Kairo, T.P. Yamaguchi, C. Brisken, A. Glick, J.J. Wysolmerski, and S.E. Millar. 2004. Canonical WNT signaling promotes

mammary placode development and is essential for initiation of mammary gland morphogenesis. *Development*. 131:4819–4829. http://dx.doi.org/10.1242/dev.01347

Cleary, A.S., T.L. Leonard, S.A. Gestl, and E.J. Gunther. 2014. Tumour cell heterogeneity maintained by cooperating subclones in Wnt-driven mammary cancers. *Nature*. 508:113–117. http://dx.doi.org/10.1038/nature13187

Connelly, J.T., J.E. Gautrot, B. Trappmann, D.W. Tan, G. Donati, W.T. Huck, and F.M. Watt. 2010. Actin and serum response factor transduce physical cues from the microenvironment to regulate epidermal stem cell fate decisions. *Nat. Cell Biol.* 12:711–718. http://dx.doi.org/10.1038/ncb2074

Creighton, C.J., A. Casa, Z. Lazard, S. Huang, A. Tsimelzon, S.G. Hilsenbeck, C.K. Osborne, and A.V. Lee. 2008. Insulin-like growth factor-I activates gene transcription programs strongly associated with poor breast cancer prognosis. *J. Clin. Oncol.* 26:4078–4085. http://dx.doi.org/10.1200/JCO.2007.13.4429

DeChiara, T.M., R.B. Kimble, W.T. Poueymirou, J. Rojas, P. Masiakowski, D.M. Valenzuela, and G.D. Yancopoulos. 2000. Ror2, encoding a receptor-like tyrosine kinase, is required for cartilage and growth plate development. *Nat. Genet.* 24:271–274. http://dx.doi.org/10.1038/73488

DiMeo, T.A., K. Anderson, P. Phadke, C. Fan, C.M. Perou, S. Naber, and C. Kuperwasser. 2009. A novel lung metastasis signature links Wnt signaling with cancer cell self-renewal and epithelial-mesenchymal transition in basal-like breast cancer. *Cancer Res.* 69:5364–5373. (published erratum appears in *Cancer Res.* 2009. 69:6366) http://dx.doi.org/10.1158/0008-5472.CAN-08-4135

Ewald, A.J., A. Brenot, M. Duong, B.S. Chan, and Z. Werb. 2008. Collective epithelial migration and cell rearrangements drive mammary branching morphogenesis. *Dev. Cell*. 14:570–581. http://dx.doi.org/10.1016/j.devcel.2008.03.003

Florian, M.C., K.J. Nattamai, K. Dörr, G. Marka, B. Uberle, V. Vas, C. Eckl, I. Andrä, M. Schiemann, R.A. Oostendorp, et al. 2013. A canonical to non-canonical Wnt signalling switch in haematopoietic stem-cell ageing. *Nature*. 503:392–396. http://dx.doi.org/10.1038/nature12631

Fuerer, C., and R. Nusse. 2010. Lentiviral vectors to probe and manipulate the Wnt signaling pathway. *PLoS ONE*. 5:e9370. http://dx.doi.org/10.1371/journal.pone.0009370

Gavin, B.J., and A.P. McMahon. 1992. Differential regulation of the Wnt gene family during pregnancy and lactation suggests a role in postnatal development of the mammary gland. *Mol. Cell. Biol.* 12:2418–2423.

Gjorevski, N., and C.M. Nelson. 2011. Integrated morphodynamic signalling of the mammary gland. *Nat. Rev. Mol. Cell Biol.* 12:581–593. http://dx.doi.org/10.1038/nrm3168

Green, J.L., T. Inoue, and P.W. Sternberg. 2007. The *C. elegans* ROR receptor tyrosine kinase, CAM-1, non-autonomously inhibits the Wnt pathway. *Development*. 134:4053–4062. http://dx.doi.org/10.1242/dev.005363

Green, J.L., T. Inoue, and P.W. Sternberg. 2008. Opposing Wnt pathways orient cell polarity during organogenesis. *Cell*. 134:646–656. http://dx.doi.org/10.1016/j.cell.2008.06.026

Green, J., R. Nusse, and R. van Amerongen. 2014. The role of Ryk and Ror receptor tyrosine kinases in Wnt signal transduction. *Cold Spring Harb. Perspect. Biol.* 6:a009175. http://dx.doi.org/10.1101/cshperspect.a009175

Grumolato, L., G. Liu, P. Mong, R. Mudbhary, R. Biswas, R. Arroyave, S. Vijayakumar, A.N. Economides, and S.A. Aaronson. 2010. Canonical and noncanonical Wnts use a common mechanism to activate completely unrelated coreceptors. *Genes Dev.* 24:2517–2530. http://dx.doi.org/10.1101/gad.1957710

Habib, S.J., B.C. Chen, F.C. Tsai, K. Anastassiadis, T. Meyer, E. Betzig, and R. Nusse. 2013. A localized Wnt signal orients asymmetric stem cell division in vitro. *Science*. 339:1445–1448. http://dx.doi.org/10.1126/science.1231077

Harterink, M., D.H. Kim, T.C. Middelkoop, T.D. Doan, A. van Oudenaarden, and H.C. Korswagen. 2011. Neuroblast migration along the anteroposterior axis of *C. elegans* is controlled by opposing gradients of Wnts and a secreted Frizzled-related protein. *Development*. 138:2915–2924. http://dx.doi.org/10.1242/dev.064733

Hatsell, S., T. Rowlands, M. Hiremath, and P. Cowin. 2003. β-catenin and Tcfs in mammary development and cancer. *J. Mammary Gland Biol. Neoplasia*. 8:145–158. http://dx.doi.org/10.1023/A:1025944723047

Herzenberg, L.A., J. Tung, W.A. Moore, L.A. Herzenberg, and D.R. Parks. 2006. Interpreting flow cytometry data: a guide for the perplexed. *Nat. Immunol.* 7:681–685. http://dx.doi.org/10.1038/ni0706-681

Ho, H.Y., M.W. Susman, J.B. Bikoff, Y.K. Ryu, A.M. Jonas, L. Hu, R. Kuruvilla, and M.E. Greenberg. 2012. Wnt5a-Ror-Dishevelled signaling constitutes a core developmental pathway that controls tissue morphogenesis. *Proc. Natl. Acad. Sci. USA*. 109:4044–4051. http://dx.doi.org/10.1073/pnas.1200421109

Huo, Y., and I.G. Macara. 2014. The Par3-like polarity protein Par3L is essential for mammary stem cell maintenance. *Nat. Cell Biol.* 16:529–537. http://dx.doi.org/10.1038/ncb2969

Ivetic, A., and A.J. Ridley. 2004. Ezrin/radixin/moesin proteins and Rho GTPase signalling in leucocytes. *Immunology*. 112:165–176. http://dx.doi.org/10.1111/j.1365-2567.2004.01882.x

Ji, H., R.J. Goode, F. Vaillant, S. Mathivanan, E.A. Kapp, R.A. Mathias, G.J. Lindeman, J.E. Visvader, and R.J. Simpson. 2011. Proteomic profiling of secretome and adherent plasma membranes from distinct mammary epithelial cell subpopulations. *Proteomics*. 11:4029–4039. http://dx.doi.org/10.1002/pmic.201100102

Kendrick, H., J.L. Regan, F.A. Magnay, A. Grigoriadis, C. Mitsopoulos, M. Zvelebil, and M.J. Smalley. 2008. Transcriptome analysis of mammary epithelial subpopulations identifies novel determinants of lineage commitment and cell fate. *BMC Genomics*. 9:591. http://dx.doi.org/10.1186/1471-2164-9-591

Kessenbrock, K., G.J. Dijkgraaf, D.A. Lawson, L.E. Littlepage, P. Shahi, U. Pieper, and Z. Werb. 2013. A role for matrix metalloproteinases in regulating mammary stem cell function via the Wnt signaling pathway. *Cell Stem Cell*. 13:300–313. http://dx.doi.org/10.1016/j.stem.2013.06.005

Khramtsov, A.I., G.F. Khramtsova, M. Tretiakova, D. Huo, O.I. Olopade, and K.H. Goss. 2010. Wnt/β-catenin pathway activation is enriched in basal-like breast cancers and predicts poor outcome. *Am. J. Pathol.* 176:2911–2920. http://dx.doi.org/10.2353/ajpath.2010.091125

Kiecker, C., and C. Niehrs. 2001. A morphogen gradient of Wnt/β-catenin signalling regulates anteroposterior neural patterning in *Xenopus*. *Development*. 128:4189–4201.

Kouros-Mehr, H., and Z. Werb. 2006. Candidate regulators of mammary branching morphogenesis identified by genome-wide transcript analysis. *Dev. Dyn.* 235:3404–3412. http://dx.doi.org/10.1002/dvdy.20978

Lim, E., D. Wu, B. Pal, T. Bouras, M.L. Asselin-Labat, F. Vaillant, H. Yagita, G.J. Lindeman, G.K. Smyth, and J.E. Visvader. 2010. Transcriptome analyses of mouse and human mammary cell subpopulations reveal multiple conserved genes and pathways. *Breast Cancer Res.* 12:R21. http://dx.doi.org/10.1186/bcr2560

Lindvall, C., N.C. Evans, C.R. Zylstra, Y. Li, C.M. Alexander, and B.O. Williams. 2006. The Wnt signaling receptor Lrp5 is required for mammary ductal stem cell activity and Wnt1-induced tumorigenesis. *J. Biol. Chem.* 281:35081–35087. http://dx.doi.org/10.1074/jbc.M607571200

Macias, H., and L. Hinck. 2012. Mammary gland development. *Wiley Interdiscip Rev Dev Biol*. 1:533–557. http://dx.doi.org/10.1002/wdev.35

Matsuda, T., M. Nomi, M. Ikeya, S. Kani, I. Oishi, T. Terashima, S. Takada, and Y. Minami. 2001. Expression of the receptor tyrosine kinase genes, Ror1 and Ror2, during mouse development. *Mech. Dev.* 105:153–156. http://dx.doi.org/10.1016/S0925-4773(01)00383-5

McCaffrey, L.M., and I.G. Macara. 2009. The Par3/aPKC interaction is essential for end bud remodeling and progenitor differentiation during mammary gland morphogenesis. *Genes Dev.* 23:1450–1460. http://dx.doi.org/10.1101/gad.1795909

Mikels, A.J., and R. Nusse. 2006. Purified Wnt5a protein activates or inhibits beta-catenin-TCF signaling depending on receptor context. *PLoS Biol.* 4:e115. http://dx.doi.org/10.1371/journal.pbio.0040115

Mikels, A., Y. Minami, and R. Nusse. 2009. Ror2 receptor requires tyrosine kinase activity to mediate Wnt5A signaling. *J. Biol. Chem.* 284:30167–30176. http://dx.doi.org/10.1074/jbc.M109.041715

Miyoshi, K., J.M. Shillingford, G.H. Smith, S.L. Grimm, K.U. Wagner, T. Oka, J.M. Rosen, G.W. Robinson, and L. Hennighausen. 2001. Signal transducer and activator of transcription (Stat) 5 controls the proliferation and differentiation of mammary alveolar epithelium. *J. Cell Biol.* 155:531–542. http://dx.doi.org/10.1083/jcb.200107065

Nalesso, G., J. Sherwood, J. Bertrand, T. Pap, M. Ramachandran, C. De Bari, C. Pitzalis, and F. Dell'accio. 2011. WNT-3A modulates articular chondrocyte phenotype by activating both canonical and noncanonical pathways. *J. Cell Biol.* 193:551–564. http://dx.doi.org/10.1083/jcb.201011051

Nelson, C.M., and M.J. Bissell. 2005. Modeling dynamic reciprocity: engineering three-dimensional culture models of breast architecture, function, and neoplastic transformation. *Semin. Cancer Biol.* 15:342–352. http://dx.doi.org/10.1016/j.semcancer.2005.05.001

Nishita, M., S. Itsukushima, A. Nomachi, M. Endo, Z. Wang, D. Inaba, S. Qiao, S. Takada, A. Kikuchi, and Y. Minami. 2010. Ror2/Frizzled complex mediates Wnt5a-induced AP-1 activation by regulating Dishevelled polymerization. *Mol. Cell. Biol.* 30:3610–3619. http://dx.doi.org/10.1128/MCB.00177-10

Oakes, S.R., H.N. Hilton, and C.J. Ormandy. 2006. The alveolar switch: coordinating the proliferative cues and cell fate decisions that drive the formation of lobuloalveoli from ductal epithelium. *Breast Cancer Res.* 8:207. http://dx.doi.org/10.1186/bcr1411

Pavlovich, A.L., E. Boghaert, and C.M. Nelson. 2011. Mammary branch initiation and extension are inhibited by separate pathways downstream of TGFβ in culture. *Exp. Cell Res.* 317:1872–1884. http://dx.doi.org/10.1016/j.yexcr.2011.03.017

Rios, A.C., N.Y. Fu, G.J. Lindeman, and J.E. Visvader. 2014. In situ identification of bipotent stem cells in the mammary gland. *Nature*. 506:322–327. http://dx.doi.org/10.1038/nature12948

Roarty, K., and R. Serra. 2007. Wnt5a is required for proper mammary gland development and TGF-β-mediated inhibition of ductal growth. *Development*. 134:3929–3939. http://dx.doi.org/10.1242/dev.008250

Saldanha, A.J. 2004. Java Treeview—extensible visualization of microarray data. *Bioinformatics*. 20:3246–3248. http://dx.doi.org/10.1093/bioinformatics/bth349

Shackleton, M., F. Vaillant, K.J. Simpson, J. Stingl, G.K. Smyth, M.L. Asselin-Labat, L. Wu, G.J. Lindeman, and J.E. Visvader. 2006. Generation of a functional mammary gland from a single stem cell. *Nature*. 439:84–88. http://dx.doi.org/10.1038/nature04372

Shore, A.N., E.B. Kabotyanski, K. Roarty, M.A. Smith, Y. Zhang, C.J. Creighton, M.E. Dinger, and J.M. Rosen. 2012. Pregnancy-induced noncoding RNA (PINC) associates with polycomb repressive complex 2 and regulates mammary epithelial differentiation. *PLoS Genet.* 8:e1002840. http://dx.doi.org/10.1371/journal.pgen.1002840

Smalley, M., and A. Ashworth. 2003. Stem cells and breast cancer: A field in transit. *Nat. Rev. Cancer*. 3:832–844. http://dx.doi.org/10.1038/nrc1212

Srinivasan, K., P. Strickland, A. Valdes, G.C. Shin, and L. Hinck. 2003. Netrin-1/neogenin interaction stabilizes multipotent progenitor cap cells during mammary gland morphogenesis. *Dev. Cell*. 4:371–382. http://dx.doi.org/10.1016/S1534-5807(03)00054-6

Stingl, J., P. Eirew, I. Ricketson, M. Shackleton, F. Vaillant, D. Choi, H.I. Li, and C.J. Eaves. 2006. Purification and unique properties of mammary epithelial stem cells. *Nature*. 439:993–997.

Stoick-Cooper, C.L., G. Weidinger, K.J. Riehle, C. Hubbert, M.B. Major, N. Fausto, and R.T. Moon. 2007. Distinct Wnt signaling pathways have opposing roles in appendage regeneration. *Development*. 134:479–489. http://dx.doi.org/10.1242/dev.001123

Takeuchi, S., K. Takeda, I. Oishi, M. Nomi, M. Ikeya, K. Itoh, S. Tamura, T. Ueda, T. Hatta, H. Otani, et al. 2000. Mouse Ror2 receptor tyrosine kinase is required for the heart development and limb formation. *Genes Cells*. 5:71–78. http://dx.doi.org/10.1046/j.1365-2443.2000.00300.x

Vafaizadeh, V., P. Klemmt, C. Brendel, K. Weber, C. Doebele, K. Britt, M. Grez, B. Fehse, S. Desriviéres, and B. Groner. 2010. Mammary epithelial reconstitution with gene-modified stem cells assigns roles to Stat5 in luminal alveolar cell fate decisions, differentiation, involution, and mammary tumor formation. *Stem Cells*. 28:928–938.

van Amerongen, R. 2012. Alternative Wnt pathways and receptors. *Cold Spring Harb. Perspect. Biol.* 4:a007914. http://dx.doi.org/10.1101/cshperspect.a007914

van Amerongen, R., and R. Nusse. 2009. Towards an integrated view of Wnt signaling in development. *Development*. 136:3205–3214. http://dx.doi.org/10.1242/dev.033910

van Amerongen, R., A. Mikels, and R. Nusse. 2008. Alternative wnt signaling is initiated by distinct receptors. *Sci. Signal.* 1:re9. http://dx.doi.org/10.1126/scisignal.135re9

van Amerongen, R., A.N. Bowman, and R. Nusse. 2012a. Developmental stage and time dictate the fate of Wnt/β-catenin-responsive stem cells in the mammary gland. *Cell Stem Cell*. 11:387–400. http://dx.doi.org/10.1016/j.stem.2012.05.023

van Amerongen, R., C. Fuerer, M. Mizutani, and R. Nusse. 2012b. Wnt5a can both activate and repress Wnt/β-catenin signaling during mouse embryonic development. *Dev. Biol.* 369:101–114. http://dx.doi.org/10.1016/j.ydbio.2012.06.020

Van Keymeulen, A., A.S. Rocha, M. Ousset, B. Beck, G. Bouvencourt, J. Rock, N. Sharma, S. Dekoninck, and C. Blanpain. 2011. Distinct stem cells contribute to mammary gland development and maintenance. *Nature*. 479:189–193. http://dx.doi.org/10.1038/nature10573

Wang, D., C. Cai, X. Dong, Q.C. Yu, X. Zhang, L. Yang, and Y.A. Zeng. 2014. Identification of multipotent mammary stem cells by protein C receptor expression. *Nature*. 517:81–84.

Wang, W., C. Jose, N. Kenney, B. Morrison, and M.L. Cutler. 2009. Global expression profiling reveals regulation of CTGF/CCN2 during lactogenic differentiation. *J. Cell Commun. Signal.* 3:43–55. http://dx.doi.org/10.1007/s12079-009-0047-5

Weber, K., U. Bartsch, C. Stocking, and B. Fehse. 2008. A multicolor panel of novel lentiviral "gene ontology" (LeGO) vectors for functional gene analysis. *Mol. Ther.* 16:698–706. http://dx.doi.org/10.1038/mt.2008.6

Welm, B.E., G.J. Dijkgraaf, A.S. Bledau, A.L. Welm, and Z. Werb. 2008. Lentiviral transduction of mammary stem cells for analysis of gene function during development and cancer. *Cell Stem Cell*. 2:90–102. http://dx.doi.org/10.1016/j.stem.2007.10.002

Williams, J.M., and C.W. Daniel. 1983. Mammary ductal elongation: differentiation of myoepithelium and basal lamina during branching morphogenesis. *Dev. Biol.* 97:274–290. http://dx.doi.org/10.1016/0012-1606(83)90086-6

Yamaguchi, T.P., A. Bradley, A.P. McMahon, and S. Jones. 1999. A Wnt5a pathway underlies outgrowth of multiple structures in the vertebrate embryo. *Development*. 126:1211–1223.

Yang, Y., L. Topol, H. Lee, and J. Wu. 2003. Wnt5a and Wnt5b exhibit distinct activities in coordinating chondrocyte proliferation and differentiation. *Development*. 130:1003–1015. http://dx.doi.org/10.1242/dev.00324

Zeng, Y.A., and R. Nusse. 2010. Wnt proteins are self-renewal factors for mammary stem cells and promote their long-term expansion in culture. *Cell Stem Cell*. 6:568–577. http://dx.doi.org/10.1016/j.stem.2010.03.020

Zhu, W., and C.M. Nelson. 2013. PI3K regulates branch initiation and extension of cultured mammary epithelia via Akt and Rac1 respectively. *Dev. Biol.* 379:235–245. http://dx.doi.org/10.1016/j.ydbio.2013.04.029